



PII S0016-7037(01)00544-0

Aqueous geochemistry of low molecular weight hydrocarbons at elevated temperatures and pressures: Constraints from mineral buffered laboratory experiments

JEFFREY S. SEEWALD*

Department of Marine Chemistry and Geochemistry, Woods Hole Oceanographic Institution, Woods Hole, MA 02543, USA

(Received June 15, 2000; accepted in revised form December 9, 2000)

Abstract—Organic matter, water, and minerals coexist at elevated temperatures and pressures in sedimentary basins and participate in a wide range of geochemical processes that includes the generation of oil and natural gas. A series of laboratory experiments were conducted at 300 to 350°C and 350 bars to examine chemical interactions involving low molecular weight aqueous hydrocarbons with water and Fe-bearing minerals under hydrothermal conditions. Mineral buffers composed of hematite-magnetite-pyrite, hematite-magnetite, and pyrite-pyrrhotite-magnetite were added to each experiment to fix the redox state of the fluid and the activity of reduced sulfur species. During each experiment the chemical system was externally modified by addition of ethene, ethane, propene, 1-butene, or *n*-heptane, and variations in the abundance of aqueous organic species were monitored as a function of time and temperature.

Results of the experiments indicate that decomposition of aqueous *n*-alkanes proceeds through a series of oxidation and hydration reactions that sequentially produce alkenes, alcohols, ketones, and organic acids as reaction intermediaries. Organic acids subsequently undergo decarboxylation and/or oxidation reactions to form carbon dioxide and shorter chain saturated hydrocarbons. This alteration assemblage is compositionally distinct from that produced by thermal cracking under anhydrous conditions, indicating that the presence of water and minerals provide alternative reaction pathways for the decomposition of hydrocarbons. The rate of hydrocarbon oxidation decreases substantially under reducing conditions and in the absence of catalytically active aqueous sulfur species. These results represent compelling evidence that the stability of aqueous hydrocarbons at elevated temperatures in natural environments is not a simple function of time and temperature alone. Under the appropriate geochemical conditions, stepwise oxidation represents a mechanism for the decomposition of low molecular weight hydrocarbons and the production of methane-rich (“dry”) natural gas.

Evaluation of aqueous reaction products generated during the experiments within a thermodynamic framework indicates that alkane-alkene, alkene-ketone, and alkene-alcohol reactions attained metastable thermodynamic equilibrium states. This equilibrium included water and iron-bearing minerals, demonstrating the direct involvement of inorganic species as reactants during organic transformations. The high reactivity of water and iron-bearing minerals suggests that they represent abundant sources of hydrogen and oxygen available for the formation of hydrocarbons and oxygenated alteration products. Thus, variations in elemental kerogen composition may not accurately reflect the timing and extent of hydrocarbon, carbon dioxide, and organic acid generation in sedimentary basins.

This study demonstrates that the stabilities of aqueous hydrocarbons are strongly influenced by inorganic sediment composition at elevated temperatures. Incorporation of such interactions into geochemical models will greatly improve prediction of the occurrence of hydrocarbons in natural environments over geologic time. Copyright © 2001 Elsevier Science Ltd

1. INTRODUCTION

Organic compounds play a fundamental role in a broad spectrum of chemical, physical and biologic processes at elevated temperatures and pressures within the earth's crust. Accumulation of oil and natural gas are obvious and economically important examples. Other examples include sediment diagenesis, the transport and deposition of ore-forming metals, and methane gas-hydrate formation. Reduced carbon compounds also represent an important source of nutrients and energy to support biologic communities that inhabit seafloor hydrothermal vent environments. Despite their significance, factors that regulate the generation and persistence of organic compounds under hydrothermal conditions are not well-understood.

In most geologic environments, organic compounds coexist with water and minerals. Numerous laboratory and theoretical studies have demonstrated that the presence of water and minerals influence organic reactions at elevated temperatures and pressures (Hoering, 1984; Tannenbaum et al., 1986; Eglinton et al., 1987; Shock, 1988; 1989; Siskin and Katritzky, 1991; Helgeson, 1991; 1999; Helgeson et al., 1993; Mango et al., 1994; Seewald, 1994; 1997; Stalker et al., 1994; Lewan, 1997; Seewald et al., 1998; McCollom and Seewald, 2001a). These studies have shown that in addition to acting as a confining medium and/or catalyst, inorganic rock components, including their aqueous pore fluids, may participate directly as reactants in reactions involving organic compounds. In addition, many organic reactions that do not occur in dry systems proceed readily in the presence of liquid water, suggesting that an aqueous solvent may facilitate specific reaction pathways. Consequently, rock composition and the

*Author to whom correspondence should be addressed (jseewald@whoi.edu).

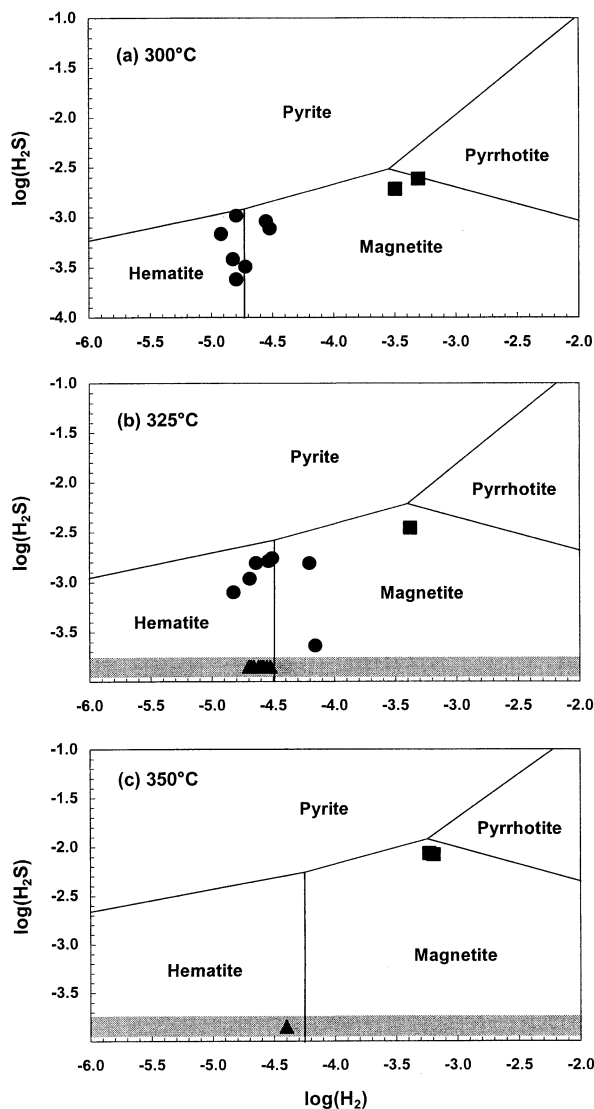


Fig. 1. Activity diagram showing phase relations in the chemical system Fe-S-O-H at (a) 300°C, (b) 325°C, and (c) 350°C and 350 bars. The symbols indicate measured $\text{H}_{2(\text{aq})}$ and $\text{H}_2\text{S}_{(\text{aq})}$ concentrations during experiments HMP (circles) and PPM (squares). The triangles in the shaded regions are plotted against the x-axis only and show measured $\text{H}_{2(\text{aq})}$ concentrations during the sulfur-free HM1 and HM2 experiments. Requisite data for the construction of this diagram are from the compilation of Johnson et al. (1992) and Toulmin and Barton (1964).

Following a reduction in temperature and an additional equilibration period, individual alkanes or alkenes were injected into the reaction cell with argon purged deionized water. Addition of water had the effect of diluting the abundance of aqueous contaminants in the reaction cell. The abundance of low molecular weight aqueous organic species were quantitatively determined as a function of time during the initial equilibration phases and after injecting organic reactants.

Four experiments, designated HMP, PPM, HM1, and HM2 to indicate the composition of the added redox buffer, were conducted at temperatures ranging from 300 to 350°C and 350 bars. During the experiments fluid composition and temperature were sequentially modified as indicated in Tables 1 to 4. Organic compounds injected into experiment HMP include ethene, ethane, propene, 1-butene, and finally *n*-heptane. During experiment PPM, *n*-heptane was the first compound injected followed by 1-butene. Ethene was the only species injected

into experiment HM1 while propene and 1-butene were sequentially injected into HM2. To investigate the effects of aqueous sulfur species on the rate and selectivity of organic reactions, a 1.01 mmolal solution of $\text{Na}_2\text{S}_2\text{O}_3$ was injected into experiment HM2 after 6049 h.

Because the aqueous phase was not completely removed before injection of new reactants during an experiment, previously injected reactants and their products persisted in solution following subsequent injections. The concentrations of these preexisting species, however, were diluted by the addition of deionized water that accompanied each injection.

2.3. Analytical Methods

The concentrations of selected aqueous species were monitored as a function of time by removing fluid aliquots from the reaction cell into glass gas-tight syringes for analysis. The first aliquot (~0.75 g) removed on any sampling occasion was discarded and served only to flush the capillary sampling line. The abundance of dissolved light hydrocarbons (C_1 - C_7) and CO_2 were determined using a purge and trap apparatus interfaced directly to a gas chromatograph equipped with serially connected thermal conductivity (TCD) and flame ionization (FID) detectors and a Porapak-Q packed column or a GSQ megabore capillary column. Injection of the fluid sample into a purge cell containing 25 wt.% phosphoric acid solution ensured complete evolution of aqueous CO_2 . A purge and trap apparatus interfaced directly to a gas chromatograph-mass spectrometer (GCMS) equipped with either a Poraplot-Q or a HP1 capillary column was used to confirm the identity of chromatographic peaks. Dissolved H_2 was determined in a separate aliquot using a gas chromatograph equipped with a TCD and a 5Å molecular sieve packed column following a headspace extraction. Dissolved alcohols and ketones were analyzed by direct splitless injection of liquid water into a gas chromatograph equipped with a FID and either a Porapak-Q packed or a Poraplot-Q capillary column. Organic acids were determined by ion chromatography using suppressed conductivity detection and either a Dionex AS11 or AS15 column. Dissolved H_2S was determined gravimetrically following acidification of the fluid with a 25 wt.% phosphoric acid solution and precipitation of evolved H_2S as Ag_2S in a 3 wt.% AgNO_3 solution. For each sampling occasion, all analyses except for H_2S were performed in duplicate. Analytical precision for all analyses is estimated at <5% (2σ) except for the $\text{H}_{2(\text{aq})}$ and $\text{H}_2\text{S}_{(\text{aq})}$ analyses which are estimated at <10% (2σ).

The concentrations of aqueous species immediately following injection of organic reactants were calculated from the measured concentrations of species before injection and the amount of water added to the reaction cell. Although much care is taken to quantitatively account for all fluid added and withdrawn during an experiment, cumulative errors introduce a degree of uncertainty with respect to the amount of water remaining in the reaction cell. This uncertainty is transferred to the calculated concentrations after each injection, but does not affect measured concentrations in subsequent samples. In addition, technical limitations associated with reactants that are gases at room temperature and pressure precluded accurate determination of the amounts injected into the reaction cell. For this reason it has been assumed that the initial concentrations of injected gaseous species are equal to or greater than the concentration in the first sample analyzed after an injection.

After the termination of each experiment, the solid products were recovered from the reaction cell and analyzed by optical microscopy and X-ray diffraction.

3. RESULTS

3.1. Dissolved H_2 and H_2S

The concentrations of dissolved $\text{H}_{2(\text{aq})}$ and $\text{H}_2\text{S}_{(\text{aq})}$ varied substantially as a function of redox buffer composition and temperature, reflecting the effectiveness of the mineral assemblages in regulating chemical conditions during the experiments (Tables 1–4, Fig. 1). X-ray diffraction analyses indicated that all buffer minerals were present at the termination of each

Table 1. Dissolved concentrations of selected aqueous species during heating with a hematite-magnetite-pyrite redox buffer (experiment HMP).

Time	Temp.	H ₂	H ₂ S	CO ₂	methane	ethane	ethene	acetate	propane	propene	acetone	propionate	<i>n</i> -butane	<i>i</i> -butane	1-butene	2-butanone			
h	°C	mm	mm	mm	μm	μm	μm	μm	μm	μm	μm	μm	μm	μm	μm	μm	μm	μm	μm
0	375	<0.001	<0.01	<0.01	<0.01	<0.01	<0.01	<1	<0.01	<0.01	<10	<1	<0.01	<0.01	<0.01	<10			
166	375	0.053	5.2	5.7	156	28	0.035	na	13	0.058	na	na	0.94	0.055	<0.01	na			
168	325	Temperature reduced to 325°C, HMP-Stage (1)																	
191	325	0.063	1.5	5.4	161	28	0.022	na	13	0.058	na	na	1.0	0.088	0.035	na			
361	325	0.070	0.2	5.3	153	30	0.049	na	14	0.20	na	na	1.6	0.20	0.37	na			
743	325	0.088	na	5.7	150	33	0.049	na	16	0.18	na	na	2.8	0.14	1.1	na			
862	325	Injected ethene and 29.9 g H ₂ O into reaction cell containing 14.1 g H ₂ O, HMP-Stage (2)																	
862	325	0.028	na	1.8	48	11	≥1.6	na	5.1	0.056	na	na	0.90	0.045	0.35	na			
908	325	0.018	na	2.3	286	18	1.5	na	7.4	0.010	na	na	1.3	0.52	<0.01	na			
1026	325	0.017	na	3.1	311	20	0.052	na	8.7	0.028	na	na	1.6	0.63	0.051	na			
1606	325	0.020	1.1	4.4	313	21	0.023	na	9.8	0.018	na	na	2.1	0.86	<0.01	na			
1703	325	Injected ethene and 14.7 g H ₂ O into reaction cell containing 27.5 g H ₂ O, HMP-Stage (3)																	
1703	325	0.013	0.7	2.9	205	14	≥76	na	6.4	0.012	na	na	1.4	0.56	<0.01	na			
1726	325	na	na	3.4	426	21	76	na	8.0	0.10	na	na	1.4	0.56	0.013	na			
1869	325	0.023	na	na	na	na	na	na	na	na	na	na	na	na	na	na			
1940	325	0.015	0.8	4.8	510	23	0.024	na	8.7	<0.01	na	na	1.7	0.64	<0.01	na			
2277	325	0.023	1.6	5.7	507	23	0.035	na	9.0	<0.01	na	na	1.8	0.66	<0.01	na			
2348	325	Injected ethane and 25.9 g H ₂ O into reaction cell containing 14.4 g H ₂ O, HMP-Stage (4)																	
2348	325	0.008	0.6	2.0	181	≥3840	0.013	na	3.2	<0.01	na	na	0.64	0.24	<0.01	na			
2396	324	0.031	1.7	2.2	197	3840	0.074	na	3.9	0.004	na	na	0.80	0.27	<0.01	na			
2948	324	0.029	1.6	2.3	192	3080	0.065	na	4.3	<0.01	na	na	1.0	0.33	<0.01	na			
3018	300	Temperature reduced to 300°C, HMP-Stage (5)																	
3047	300	0.021	na	2.4	193	3370	0.035	na	4.6	0.006	na	na	1.1	0.49	<0.01	na			
3067	300	na	na	2.4	199	3400	nd	na	4.6	0.010	na	na	1.0	0.49	<0.01	na			
3238	300	na	na	2.5	196	3270	0.019	na	4.9	0.020	na	na	1.2	0.63	<0.01	na			
3408	300	Injected ethene and 28.1 g H ₂ O into reaction cell containing 13.6 g H ₂ O, HMP-Stage (6)																	
3408	300	na	na	0.81	64	1065	≥189	na	1.6	0.007	na	na	0.39	0.21	<0.01	na			
3428	299	na	na	0.86	94	990	189	na	2.5	0.060	na	na	0.62	0.36	0.025	na			
3525	299	0.012	0.7	1.0	110	1000	0.16	na	2.7	0.013	na	na	0.71	0.42	<0.01	na			
5133	300	0.015	0.4	2.4	125	1065	0.010	na	4.4	0.006	na	na	1.4	0.85	<0.01	na			
7820	299	0.019	0.3	3.2	138	1040	0.007	na	4.5	0.004	na	na	1.3	0.58	<0.01	na			
7846	299	Injected propene and 17.7 g H ₂ O into reaction cell containing 24.6 g H ₂ O, HMP-Stage (7)																	
7846	299	0.010	0.2	1.7	75	566	0.004	na	2.5	≥16	na	na	0.71	0.32	<0.01	na	2-propanol	na	
7916	299	0.033	na	2.1	79	566	0.050	na	46	16	na	na	0.75	0.34	0.028	na		<100	
8013	301	0.030	na	2.5	80	613	0.027	na	46	0.25	1750	na	0.79	0.26	nd	<10		<100	
8443	299	0.032	na	3.9	81	596	0.020	na	45	0.070	662	na	0.87	0.43	nd	<10		<100	
11301	300	0.030	0.8	7.6	91	613	0.025	176	42	0.005	<10	<1	1.5	0.74	0.064	<10		<100	
11615	300	Injected propene and 24.5 g H ₂ O into reaction cell containing 11.8 g H ₂ O, HMP-Stage (8)																	
11615	300	0.009	na	2.2	27	179	0.007	51	12	≥1200	<10	<1	0.44	0.22	0.019	<10		<100	
11636	300	0.043	na	2.4	42	179	0.93	309	378	1200	7850	313	0.94	0.74	0.059	<10		1680	
11707	299	0.036	na	3.7	45	191	0.17	1390	383	26	9150	479	0.92	0.55	1.2	<10		<100	
12022	299	0.044	na	10	51	198	0.092	4850	382	0.75	4830	191	1.1	1.7	2.5	<10		<100	
13029	299	0.045	na	24	67	195	0.022	3850	366	0.10	473	BD	1.2	3.2	<0.01	<10		<100	
19321	300	0.046	na	na	86	198	0.003	2	321	0.021	<10	3	2.5	1.6	<0.01	<10		<100	
19364	299	na	na	33	87	199	0.021	na	297	0.031	na	na	2.6	1.8	<0.01	<10		na	
19415	299	Injected 1-butene and 32.7 g H ₂ O into reaction cell containing 7.4 g H ₂ O, HMP-Stage (9)																	
19415	300	na	na	5.3	14	32	0.003	na	48	0.005	na	na	0.42	0.3	≥30	<10		butyrate	isobutyrate
19437	301	0.020	na	5.6	23	32	0.063	170	53	0.45	<10	7	74	na	30.4	240		<5	<5
19510	300	na	na	5.6	29	32	0.019	330	54	0.46	<10	27	5.6	0.37	1.1	294		<5	<5
19605	301	0.017	na	5.9	31	33	0.029	502	55	0.29	<10	46	3.1	0.51	0.005	181		<5	<5
19918	300	0.017	na	6.1	32	34	0.015	599	55	0.11	<10	30	3.2	0.60	0.002	17		6	33
20063	300	Injected ethene and 17.0 g H ₂ O into reaction cell containing 19.3 g H ₂ O, HMP-Stage (10)																	
20063	300	na	na	3.2	17	18	≥2060	319	29	0.059	<10	16	1.7	0.32	<0.01	9		<100	<100
20085	300	na	na	4.3	377	73	2060	13300	62	4.7	467	<1	4.6	0.26	<0.01	<10		1020	1230
20204	299	na	na	6.7	425	84	1.0	16800	64	0.073	134	<1	3.0	0.44	<0.01	<10		<100	<100
23037	299	0.016	0.2	na	na	na	na	2910	na	na	<10	<1	na	na	<0.01	<10		<100	<100
23085	299	na	na	35	627	92	0.018	na	67	0.012	na	<1	3.4	0.82	<0.01	<10		na	na

na = not analyzed
mm = mmolal
μm = μmolal

Table 2. Dissolved concentrations of selected aqueous species during heating of *n*-heptane with a hematite-magnetite-pyrite and a pyrite-pyrrhotite-magnetite mineral assemblage.

Time h	Temp. °C	H ₂ mm	H ₂ S mm	CO ₂ mm	methane μm	ethane μm	propane μm	<i>n</i> -butane μm	<i>i</i> -butane μm	<i>n</i> -pentane μm	<i>n</i> -hexane μm	heptane mm	ethene μm	propene μm	1-butene μm	acetate μm	propionate μm	butyrate μm	isobutyrate μm	valerate μm	caproate μm
Experiment HMP*																					
23135 299 Injected <i>n</i> -heptane and 20.4 g H ₂ O into reaction cell containing 14.3 g H ₂ O, HMP-Stage (11)																					
23135	299	0.006	na	0.08	12	220	32	24	1.2	0.29	0.69	0.12	1.9 [†]	0.006	0.004	<0.01	1020	<1	<1	<1	<1
23206	299	0.016	na	14	251	33	26	1.3	0.30	0.77	1.2	0.86	0.030	0.011	<0.01	1020	<1	<1	<1	<1	<1
24117	299	0.016	1.0	16	219	33	25	2.0	0.11	0.70	2.6		0.026	0.006	0.66	620	<1	<1	<1	<1	<1
24142 299 Injected <i>n</i> -heptane and 22.2 g H ₂ O into reaction cell containing 14.7 g H ₂ O, HMP-Stage (12)																					
24142	299	0.006	0.4	5.7	81	12	9.2	0.74	0.042	0.95	128 [†]		0.010	0.002	0.24	228	<1	<1	<1	<1	<1
24212	300	na	na	5.7	123	45	35	28	0.26	12	5.0	104	0.30	2.6	2.3	353	28	23	<1	14	10
24574	299	0.024	na	7.9	176	183	146	138	2.2	22	13	146	0.030	2.8	2.9	1280	187	140	40	63	39
26589	299	0.021	na	45	458	838	721	708	22	59	31	151	0.38	4.1	na	7690	418	404	332	173	109
27622	299	0.028 [‡]	0.9	82	605	1040	784	679	36	64	27	76	0.89	14	13	10500	483	41	470	148	91
Experiment PPM																					
0	375	<0.001	<0.01	<0.01	<0.01	<0.01	<0.01	<0.01	<0.01	<0.01	<0.01	<0.01	<0.01	<0.01	<0.01	<1	<1	<1	<1	<1	<1
505	300	Temperature reduced to 300°C, PPM-Stage (1)																			
533	301	0.36	na	1.9	133	32	32	5.9	3.0	0.78	0.15		0.032	0.11	<0.01	32	<1	1	<1	<1	<1
630 299 Injected <i>n</i> -heptane and 19.9 g H ₂ O into reaction cell containing 27.5 g H ₂ O, PPM-Stage (2)																					
630	299	0.26	na	1.1	77	19	19	3.4	1.7	0.45	0.09	12.7 [†]	0.019	0.062	<0.01	19	<1	<1	<1	<1	<1
700	299	0.31	na	1.1	82	22	16	5.6	2.0	2.0	0.27	1.7	0.17	0.41	<0.01	30	5	3	<1	<1	<1
942	299	0.30	na	1.1	118	52	38	14	7.0	3.9	0.40	2.7	0.089	0.26	<0.01	63	na	na	na	na	na
1371	299	0.31	na	1.2	155	82	57	21	10	5.3	0.57	3.0	0.084	0.33	<0.01	43	9	8	<1	<1	<1
2859	299	0.32	1.9	1.3	252	161	118	55	24	15	9.4	5.0	0.10	0.80	<0.01	90	36	44	3	5	1
3652	300	0.31	na	1.5	304	199	144	68	29	20	13	5.2	0.092	1.2	<0.01	na	na	na	na	na	na

na = not analyzed

mm = mmolal

μm = μmolal

*The data shown here are from a continuation of experiment HMP. See Table 1 for stages (1)–(10).

[†]Calculated from the amount of *n*-heptane injected. See text for details.

[‡]Values from sample taken at 27167 h.

Table 3. Dissolved concentrations of selected aqueous species during heating with a pyrite-pyrrhotite-magnetite mineral assemblage (experiment PPM).*

Time [†] h	Temp. °C	H ₂ mm	H ₂ S mm	CO ₂ mm	methane μm	ethane μm	ethene μm	acetate μm	propane μm	propene μm	acetone μm	propionate μm	n- butane μm	i- butane μm	1- butene μm	2- butanol μm	2- butanone μm	butyrate μm	isobutyrate μm	n- heptane mm
3679	300	Injected 1-butene and 27.1 g H ₂ O into reaction cell containing 13.9 g H ₂ O, PPM-Stage (3)																		
3679	300	0.011	na	0.51	103	67	0.031	na	49	0.41	na	na	23	10	≥65600	<80	na	na	na	1.8
3699	300	0.92	na	0.58	128	88	3.6	230	83	5.6	144	30	nd	nd	65600 [‡]	17900	79300	403	60	3.5
3797	300	0.49	2.4	0.82	160	105	2.4	477	114	2.5	422	95	8100	90	470	80	142000	1090	374	2.5
4059	300	0.37	na	1.7	277	183	2.5	973	182	6.9	1410	303	9600	200	310	<80	135000	1660	542	2.2
4708	299	0.34	na	4.3	470	292	2.1	2590	306	16	3920	1010	13000	380	nd	<80	120000	3040	970	1.9
4732	325	Heated to 325°C and injected 25.3 g H ₂ O into reaction cell containing 15.2 g H ₂ O, PPM-Stage (4)																		
4732	325	0.13	na	1.6	177	110	0.79	974	115	0.38	1474	380	4887	109	nd	<80	45113	1143	365	0.71
4802	324	0.47	na	2.1	241	148	3.8	1300	179	10	1790	453	5730	211	310	<80	44900	1230	387	0.82
5741	324	0.43	na	8.6	709	373	3.0	2920	553	22	5050	1440	6150	561	nd	<80	32100	2120	913	0.60
6409	324	0.42	3.5	14	1030	540	2.8	4500	1000	28	6440	2000	7920	880	nd	<80	23900	2500	1190	0.64
6481	350	Heated to 350°C and injected 18.1 g H ₂ O into reaction cell containing 22.3 g H ₂ O, PPM-Stage (5)																		
6481	350	0.23	1.9	7.7	569	298	1.5	2486	552	15	3558	1105	4376	486	nd	<80	13204	1381	657	0.35
6506	348	0.59	na	8.6	664	360	7.1	3030	710	22	3780	1110	5510	647	nd	<80	12600	1290	667	0.50
6653	349	0.60	na	12	989	557	7.5	3600	977	25	4600	1060	6470	814	nd	<80	11800	1800	709	0.57
7541	349	0.59	8.5	29	2380	1170	4.5	5050	1830	25	5450	707	4560	897	nd	<80	5360	250	580	0.21
11620	349	0.64	8.3	61	5630	2390	1.9	2610	3760	9.1	2150	245	3820	908	nd	<80	858	40	140	0.070

na = not analyzed

nd = no data due to coelution of chromatographic peaks

mm = mmolal

μm = μmolal

*The data shown here are from a continuation of experiment PPM (Table 2).

[†]Time from initial heating. See Table 2 for stages (1) and (2) of this experiment.[‡]Reported value is the sum of all possible butene isomers.

experiment. Reaction of PPM at 325°C resulted in H_{2(aq)} and H_{2S(aq)} concentrations of approximately 0.4 and 4 mmolal, respectively, compared with 0.03 and 1 mmolal during the HMP experiment. In general, measured concentrations of H_{2(aq)} and H_{2S(aq)} were consistent with values predicted from thermodynamic data for reactions (1)–(4) indicating attainment of thermodynamic equilibrium (Fig. 1). These data clearly indicate that for a given temperature, PPM equilibrium produced a more reducing environment with higher H_{2S(aq)} activity relative to equilibration of HMP and HM. The rapid return of H_{2(aq)} and H_{2S(aq)} concentrations to equilibrium values following perturbation of the chemical system either by injection of H₂- and H₂S-free water or temperature change indicates that the rates of mineral reactions were sufficiently rapid to buffer the chemical environment despite other redox dependent reactions involving aqueous organic species.

Following injection of Na₂S₂O₃ into experiment HM2, the presence of H₂S in fluid samples was confirmed by its strong characteristic odor. Absolute H₂S concentrations, however, can only be constrained to ≤0.5 mmolal due to the relatively high detection limits associated with the gravimetric method used for hydrogen sulfide determinations.

3.2. Aqueous Organic Compounds

3.2.1. Hematite-magnetite-pyrite experiment

Reaction of alkenes and alkanes with the HMP mineral assemblage produced large and rapid changes in fluid composition (Tables 1 and 2, Figs. 2 and 3). Ethene abundance decreased rapidly following injection at 300°C and resulted in the production of a variety of alteration products including

methane, ethane, ethanol, acetaldehyde, acetic acid, and carbon dioxide. Except for carbon dioxide, all oxygenated organic alteration species underwent secondary reactions and initial increases in concentration during the early stages of reaction were followed by decreases. Although the absolute amount of ethene injected could not be determined, constant mass balance on total carbon in later fluid samples suggests that all major alteration products were identified (Fig. 2a). The abundances of oxygenated organic alteration products were not determined following ethene injection at 325°C. Generation of methane, ethane, and carbon dioxide, however, indicates the occurrence of reactions similar to those during the 300°C phase of the experiment (Table 1).

Reaction following injection of ethane at 325°C resulted in the production of ethene and carbon dioxide and consumption of ethane (Fig. 2b). In contrast to increasing concentrations following ethene injection, methane abundance remained constant. Poor mass balance on total aqueous carbon indicates the presence of species not accounted for during this experiment (Fig. 2b). Ethanol, acetaldehyde, and acetic acid, which were not analyzed, represent likely candidates. Reducing temperature from 325 to 300°C resulted in decreased ethene abundance. Methane and carbon dioxide concentrations remained constant while the ethane concentration increased slightly.

Propene abundance decreased rapidly following injection at 300°C and produced a product assemblage that included relatively minor quantities of methane, ethane, and propionic acid, in addition to more abundant propane, 2-propanol, acetone, acetic acid, and carbon dioxide (Fig. 2c). Except for carbon dioxide, methane, and ethane, all other products underwent secondary reactions resulting in decreased concentrations dur-

Table 4. Dissolved concentrations of selected aqueous species during heating with a hematite-magnetite mineral assemblage.

Time h	Temp. °C	H ₂ mm	H ₂ S mm	CO ₂ mm	methane μm	ethane μm	ethene μm	ethanol μm	acetate μm	propane μm	propene μm	acetone μm	propionate μm	2- propanol μm	<i>n</i> - butane μm	<i>i</i> - butane μm	1- butene μm	2- butanone μm	2- butanol μm
Experiment HM1																			
0	326	<0.001	<0.01	<0.01	<0.01	<0.01	<0.01	<100	<10	<0.01	<0.01	<10	<100	<100	<0.01	<0.01	<0.01	<100	<100
99	326	0.026	<0.01	4.5	6.3	1.2	0.17	na	na	0.96	1.2	na	na	na	na	na	na	na	na
145	326	0.026	<0.01	4.4	6.2	1.3	0.16	na	na	0.85	1.4	na	na	na	na	na	na	na	na
171	325	Injected ethene and 16.7 g H ₂ O into reaction cell containing 21.5 g H ₂ O, HM1-Stage (1)																	
171	325	na	<0.01	2.5	3.5	0.73	≥283	na	na	0.48	0.8	na	na	na	na	na	na	na	na
222	326	na	<0.01	2.8	6.2	2.4	283	na	na	0.67	1.0	na	na	na	na	na	na	na	na
243	326	0.020	<0.01	na	na	na	na	na	na	na	na	na	na	na	na	na	na	na	na
288	326	na	<0.01	2.7	8	3.7	174	na	na	1.0	1.1	na	na	na	na	na	na	na	na
335	326	na	<0.01	2.7	10	5.3	156	na	na	0.78	1.0	na	na	na	na	na	na	na	na
406	326	na	<0.01	na	na	na	na	411	na	na	na	na	na	na	na	na	na	na	na
Experiment HM2																			
0	350	<0.001	<0.01	<0.01	<0.01	<0.01	<0.01	<100	<10	<0.01	<0.01	<10	<1	<100	<0.01	<0.01	<0.01	<10	<100
385	347	0.040	<0.01	na	na	na	na	na	na	na	na	na	na	na	na	na	na	na	na
389	325	Lowered T to 325°C, HM2-Stage (1)																	
412	325	NA	<0.01	4.6	81	47	3.1	<100	444	30	27	101	10	na	48	na	49	37	<100
581	325	0.030	<0.01	4.6	88	50	2.3	<100	442	32	25	114	9	<100	47	na	56	43	<100
677	325	Injected propane and 22.9 g H ₂ O into reaction cell containing 15.3 g H ₂ O, HM2-Stage (2)																	
677	325	0.012	<0.01	1.8	35	20	0.92	<100	177	13	≥2240	46	4	<100	19	na	22	17	<100
771	325	0.025	<0.01	2.1	46	23	1.2	<100	221	64	2240	347	44	1960	20	na	25	20	<100
3773	325	0.021	<0.01	3.8	143	58	1.2	<100	825	206	146	2840	24	<100	73	28	58	83	<100
4111	325	Injected 1-butene and 23.2 g H ₂ O into reaction cell containing 21.5 g H ₂ O, HM2-Stage (3)																	
4111	325	0.010	<0.01	1.8	69	28	0.58	<100	402	99	70	1365	12	<100	35	13	≥923 [†]	40	<100
4179	325	0.020	<0.01	1.9	72	34	0.79	<100	431	97	50	1390	11	<100	nd	nd	923 [†]	61	182
4782	325	0.025	<0.01	2.3	92	37	0.98	<100	459	106	46	1400	16	<100	nd	nd	489 [†]	155	<100
5979	325	0.028	<0.01	2.8	131	49	0.85	<100	563	119	33	1410	17	<100	nd	nd	383 [†]	269	<100
6049	325	Injected 1.01 mmolal Na ₂ S ₂ O ₃ and 25.4 g H ₂ O into reaction cell containing 16.5 g H ₂ O, HM2-Stage (4)																	
6049	325	0.011	P	1.1	52	19	0.34	<100	222	47	13	555	7	<100	nd	nd	151 [†]	106	<100
6074	325	0.022	P	1.1	57	22	0.46	<100	257	51	12	535	10	<100	nd	nd	164 [†]	107	<100
6245	325	0.022	P	1.3	99	50	1.7	<100	369	83	13	481	22	<100	69	48	1.1	94	<100
6747	325	0.024	P	2.1	164	79	2.9	<100	653	122	8.3	345	25	<100	63	101	1.5	50	<100

na = not analyzed

nd = no data due to coelution of chromatographic peaks

mm = mmolal

μm = μmolal

P = presence confirmed by odor

[†]Reported value is the sum of all possible butene isomers.

ing the later stages of reaction. Mass balance on total aqueous carbon indicates a small decrease with continued reaction that is difficult to distinguish from the analytical uncertainty, but may suggest the presence of unidentified alteration products at relatively low concentrations (Fig. 2c).

Injection of 1-butene at 300°C produced trends similar to the propene experiment that involved a corresponding assemblage of C₄ alteration products (Fig. 2d). Rapid reaction of 1-butene resulted in the generation of *n*-butane, 2-butanone, acetic acid, carbon dioxide and minor methane. Mass balance on total aqueous carbon indicates that the majority of alteration products were accounted for during this experiment (Fig. 2d).

The first attempt at injecting *n*-heptane into experiment HMP resulted in an exceedingly low aqueous concentration of this compound (HMP-stage 11; Table 2). Because the abundance of *n*-heptane alteration products after this initial injection were insignificant relative to the concentrations of organic species preexisting in the reaction cell, a second aliquot of *n*-heptane was injected at 24142 h (HMP-stage 12; Table 2). As might be expected, reaction of longer chain aqueous *n*-heptane in the presence of HMP produced an assemblage of alteration products with significantly greater compositional diversity than the shorter chain reactants (Table 2, Fig. 3). Ethane was the most abundant *n*-alkane generated followed by propane, *n*-butane, and methane in order of decreasing abundance in addition to

relatively minor amounts of *i*-butane, *n*-pentane and *n*-hexane. Based on the amount of *n*-heptane injected into the reaction cell during HMP-stage 12, the calculated initial *n*-heptane concentration was 128 mmolal, a value that is generally consistent with the measured concentrations that varied from 76 to 151 mmolal. This concentration range is below the aqueous solubility at 300°C and 350 bars, but exceeds the saturation limit at 25°C and 1 bar (Price 1981). Accordingly, the non-systematic trends in the observed *n*-heptane concentrations likely reflect exsolution of *n*-heptane on the walls of the sampling tube and valve in response to cooling during fluid withdrawal. Because previously condensed *n*-heptane could be swept into the sampling syringe during removal of subsequent replicate samples, measured errors in the reported values are both positive and negative. The large uncertainties associated with the measured *n*-heptane concentrations preclude meaningful total mass balance on aqueous carbon during this experiment. Mass balance on the analyzed alteration products, however, indicates that a minimum of 12.7% of the initial 128 mmolal *n*-heptane decomposed during this phase of the experiment.

In addition to saturated hydrocarbons, C₂-C₆ carboxylic acid anions were generated during *n*-heptane decomposition. The concentration of acetic acid exceeded that of the other acids by more than an order of magnitude attaining a concentration of 10.5 mmolal after 3480 h (Table 2). Carbon dioxide was by far

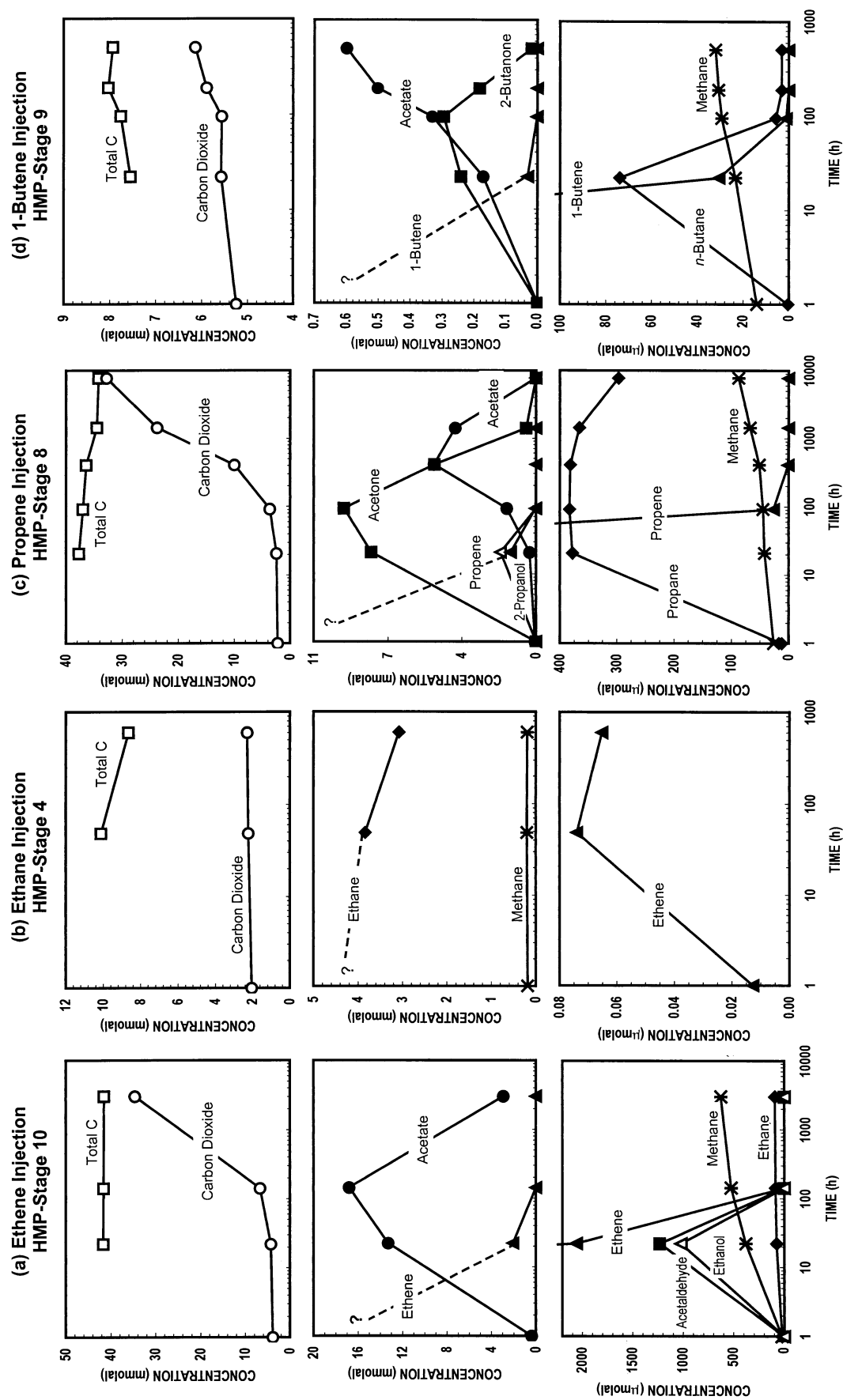


Fig. 2. Variations in the concentrations of selected aqueous species during heating of (a) ethane at 300°C, (b) ethane at 325°C, (c) propene at 300°C, and (d) 1-butene at 300°C in the presence of a hematite-magnetite-pyrite redox buffer (experiment HMP). The data are plotted as a function of time elapsed since injection of each reactant into the reaction cell.

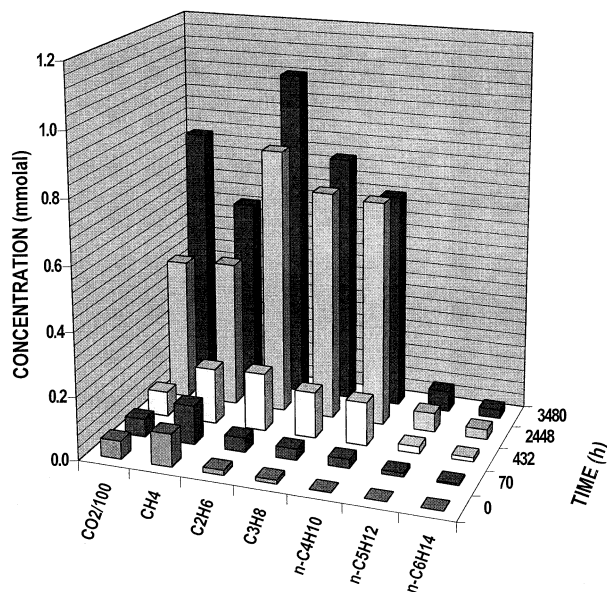


Fig. 3. Variations in the concentrations of selected aqueous species as a function of time during heating of *n*-heptane at 300°C in the presence of a hematite-magnetite-pyrite redox buffer (HMP-Stage 12). The data are plotted as a function of time elapsed since injection of *n*-heptane into the reaction cell.

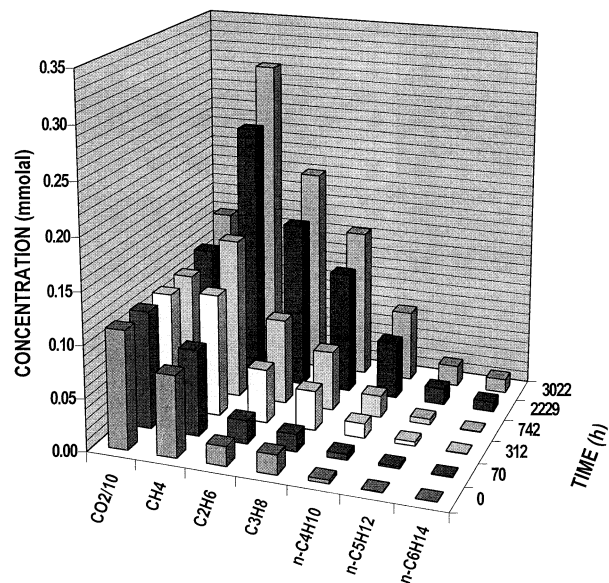


Fig. 4. Variations in the concentrations of selected aqueous species as a function of time during heating of *n*-heptane at 300°C in the presence of a pyrite-pyrrhotite-magnetite redox buffer (PPM-Stage 2). The data are plotted as a function of time elapsed since injection of *n*-heptane into the reaction cell.

the most abundant alteration product, however, reaching a final concentration of 82 mmolal. This value is almost an order of magnitude higher than the 1.04 mmolal ethane which was the most abundant saturated hydrocarbon product. Qualitative GCMS analysis indicated the presence of equimolar amounts of 2-heptanone, 3-heptanone, and 4-heptanone in solution. Analysis of C_7 alkene isomers was hindered by co-elution of the extremely large *n*-heptane peak during chromatographic separation. Nonetheless aqueous 2-heptene was positively identified by GCMS. The results of qualitative GCMS analysis indicate that increasing amounts of toluene and benzene formed with continued reaction during the experiment.

3.2.2. Pyrite-pyrrhotite-magnetite experiment

Decomposition of aqueous *n*-heptane at 300°C in the presence of the PPM buffer produced an aqueous alteration assemblage that contained the same compounds as were observed during *n*-heptane decomposition in the presence of the HMP buffer, but at different relative abundances. For example, in contrast to the HMP experiment, methane was the most abundant saturated hydrocarbon produced followed by ethane, propane, *n*-butane, *i*-butane, *n*-pentane, and *n*-hexane in order of decreasing abundance (Table 2, Fig. 4). The amounts of *n*-pentane and *n*-hexane generated were significantly less than the shorter chain *n*-alkanes resulting in a sharp deflection in the trend of increasing hydrocarbon abundance with decreasing chain length, as was observed during the HMP experiment (Fig. 5). The molal amounts of carbon dioxide produced were similar to the *n*-alkanes. Other oxygenated products identified included C_2 - C_6 carboxylic acids and all possible C_7 ketone isomers.

The calculated aqueous *n*-heptane concentration following injection during experiment PPM is 12.7 mmolal, a value that

exceeds the aqueous solubility at 25°C and 1 bar and suggests the measured abundances of *n*-heptane may not accurately reflect concentrations inside the reaction cell due to exsolution during sampling. Mass balance on the analyzed alteration products indicates 2.5% of the initial *n*-heptane decomposed during this experiment, a value significantly lower than the 12.7% during the HMP experiment. Assuming that the rate of *n*-heptane decomposition is first order or greater with respect to *n*-heptane concentration, these results indicate faster decomposition reactions in the presence of HMP relative to PPM.

Following the *n*-heptane phase of the experiment, injection of 1-butene into the reaction cell at 300°C resulted in rapid reaction to initially form 2-butanol, 2-butanone, and *n*-butane (Table 3, Fig. 6). GCMS analysis indicated rapid isomerization of 1-butene to produce all possible butene isomers before withdrawal of the first fluid sample. Subsequent reactions resulted in the disappearance of 2-butanol and decreasing concentrations of 2-butanone, while *n*-butane continued to increase in abundance along with carbon dioxide, methane, ethane, propane, *i*-butane, and acetone. Butyric acid was the most abundant carboxylic acid generated at 300°C, followed by acetic, propanoic, and isobutyric acid in order of decreasing abundance. Mass balance on total aqueous carbon during the 300°C phase of the experiment indicates decreasing abundance with time (Fig. 6). This trend may reflect sampling related artifacts due to aqueous butene and *n*-butane concentrations that exceeded their aqueous solubilities at 25°C and 1 bar.

Reactions following the increase in temperature to 325°C while at the same time injecting deionized water did not change the relative abundance of generated products significantly except for a large increase in the relative abundance of acetic acid. A subsequent temperature increase to 350°C and injection of deionized water, however, resulted in decomposition of many

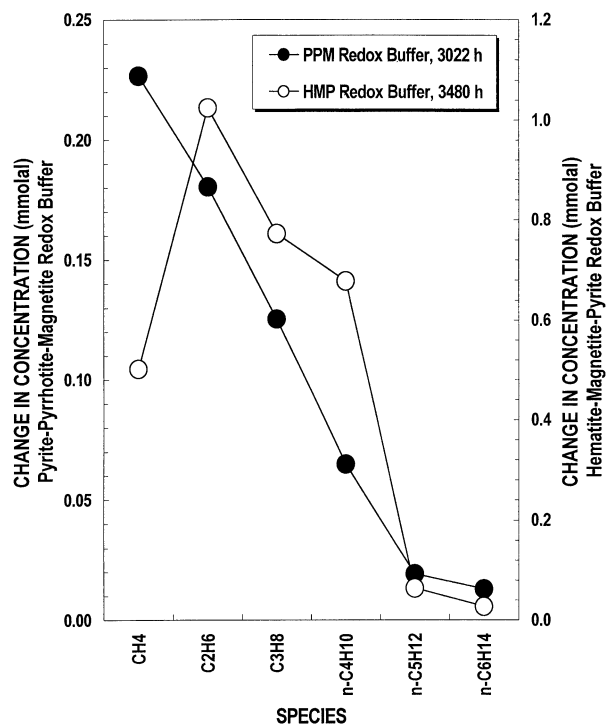


Fig. 5. Change in concentration of aqueous C_1 - C_6 *n*-alkanes during heating of *n*-heptane in the presence of a pyrite-pyrrhotite-magnetite redox buffer for 3022 h (PPM-Stage 2, solid circles, left axis) and a hematite-magnetite-pyrite redox buffer for 3480 h (HMP-Stage 12, open circles, right axis). The change in concentration is calculated as the difference in measured concentration at the time of sampling and at the time of *n*-heptane injection.

alteration products that were generated during the earlier lower temperature stages of reaction. In addition to acetone, 2-butanone, and *n*-butane, all organic acids decreased in concentration after 5139 h of reaction at 350°C, while C_1 - C_3 saturated hydrocarbons and carbon dioxide abundances increased.

3.2.3. Hematite-magnetite experiments

The composition and temporal variations in the concentrations of aqueous alteration products during experiments HM1 and HM2 were generally similar to experiment HMP, although the rates of individual reactions were considerably slower (Table 4, Fig. 7). In particular, injected alkenes persisted at concentrations considerably higher than their corresponding *n*-alkanes for thousands of hours during experiments HM1 and HM2 in contrast to the HMP experiment where relatively fast reaction resulted in rapidly decreasing concentrations to levels below those of corresponding *n*-alkanes. Ethene injection into experiment HM1 was accompanied by the slow production of ethane and methane and substantially higher concentrations of ethanol. The abundance of other species such as acetic acid and acetaldehyde were not measured during this experiment. Injection of propene into experiment HM2 resulted in the formation of 2-propanol which subsequently decomposed to produce acetone, acetic acid, carbon dioxide, methane and propane (Fig. 7). Injection of 1-butene was followed initially by the production of 2-butanone which decreased in abundance with continued

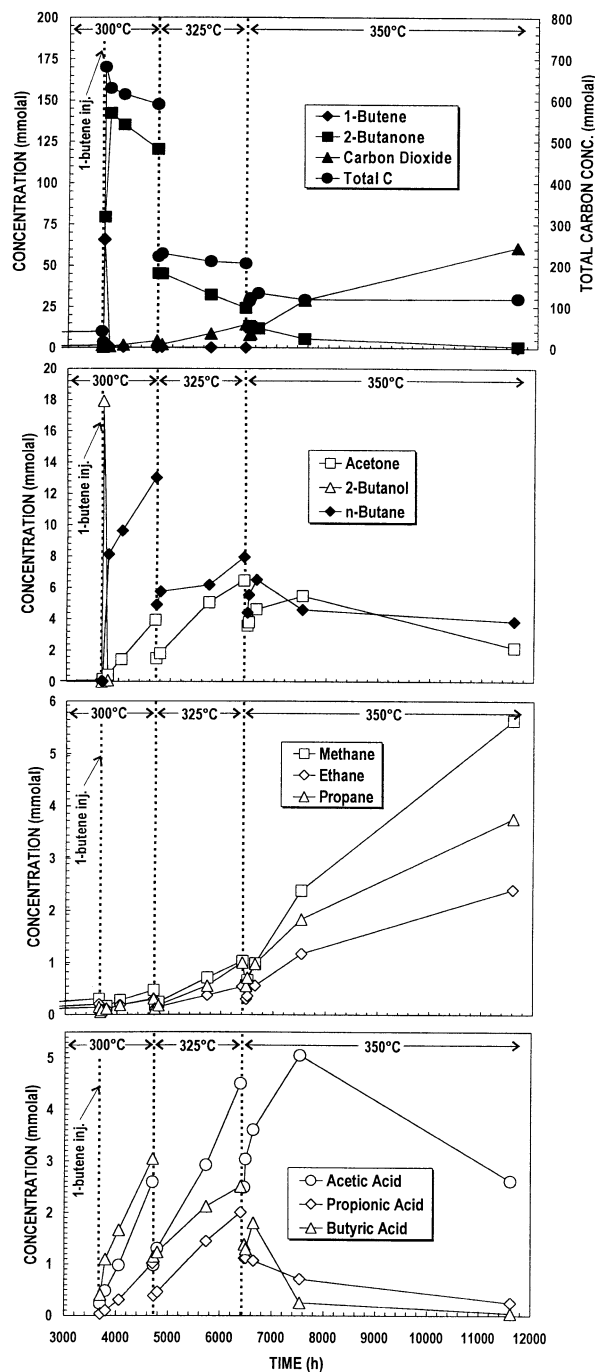


Fig. 6. Variations in the concentration of selected aqueous species during heating of 1-butene in the presence of a pyrite-pyrrhotite-magnetite redox buffer (experiment PPM). The temperature of the experiment was initially 300°C (PPM-Stage 3) but was subsequently increased to 325°C (PPM-Stage 4) and 350°C (PPM-Stage 5) at the indicated times. Injection of argon-purged deionized water accompanied the addition of 1-butene and subsequent temperature increases resulting in decreased concentrations of preexisting aqueous species.

reaction. Other products included 2-butanone, acetic acid, carbon dioxide and methane. Rapid isomerization of 1-butene resulted in the formation of all stable *n*-butenes in near equal amounts. Reaction rates increased dramatically following ad-

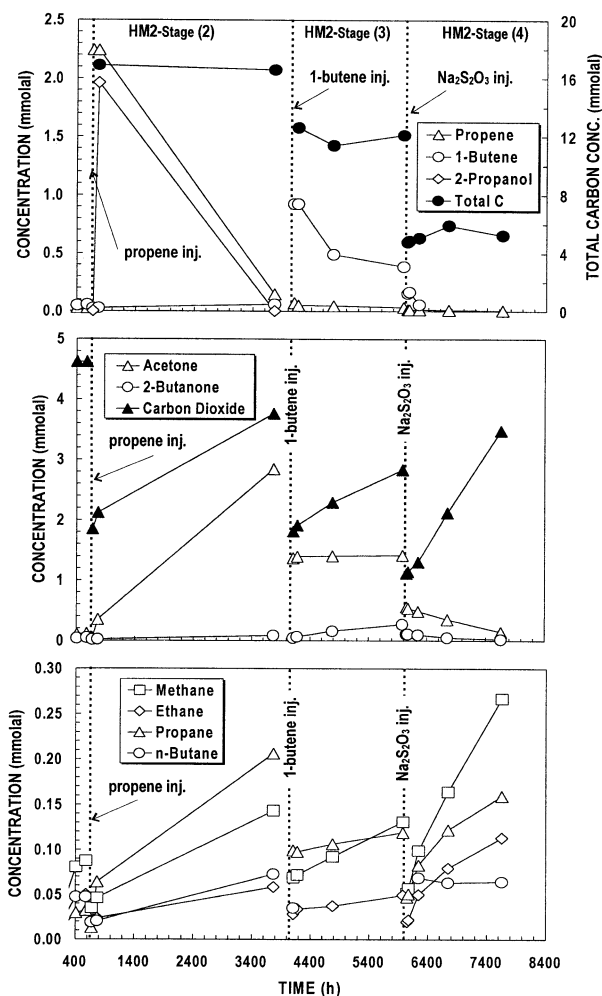


Fig. 7. Variations in the concentration of selected aqueous species during heating of propene and 1-butene in the presence of a hematite-magnetite redox buffer (experiment HM2) at 325°C. Propene was injected at 677 h, 1-butene at 4111 h, and Na₂S₂O₃ at 6049 h.

dition of Na₂S₂O₃ to the system, resulting in rapid methane, ethane, propane and *n*-butane production and rapid decreases in the abundance of *n*-butenes (Fig. 7). Constant total carbon mass balance during experiment HM2 suggests that the majority of carbon species present were analyzed.

4. DISCUSSION

4.1. Reaction Pathways

Results of the experiments indicate that aqueous alkane and alkene decomposition at elevated temperatures and pressures follows a reaction path that involves reduction, oxidation, and hydration. Some of these transformations involve parallel processes while others are clearly sequential. Ethene reduction in the presence of HMP at 300°C, for example, resulted in the rapid production of ethane while simultaneous hydration followed by oxidation produced oxygenated products. Temporal variations in the appearance and disappearance of reaction products suggests that ethene initially undergoes a hydration step to form ethanol, which is sequentially oxidized to acetal-

dehyde, acetic acid, and finally CO₂ (Fig. 2a). This sequence of reactions is shown schematically in Figure 8a. Although the abundances of all oxygenated products were not determined following ethene injection at 325°C, the rapid decomposition of ethene accompanied by the production of CO₂ and ethane suggests similar processes were occurring at this higher temperature.

In general, reaction of propene and 1-butene at 300°C in the presence of HMP occurred via a sequence of reactions that were similar to ethene decomposition (Figs. 8b,c). Hydration of propene resulted in the production of 2-propanol which was subsequently oxidized to acetone. The absence of significant amounts of 1-propanol and propionaldehyde indicates that these hydration and oxidation reactions are specific to the interior carbon of the double bond. Reaction of 1-butene in the presence of the HMP and PPM redox buffers at 300°C was characterized by the same specificity favoring the formation of 2-butanone over butyraldehyde. Measurable quantities of 2-butanol during the early stages following 1-butene injection into experiment PPM suggest that this reaction proceeded through an alcohol intermediary. The abundance of 2-butanol was below detection during the HMP experiment, a likely result of oxidation to form 2-butanone at a rate sufficiently rapid to preclude accumulation in solution. Addition of hydroxyl to the interior carbon of double bonds (Markovnikov addition) suggests that hydration reactions may involve an ionic mechanism (Streitwieser and Heathcock, 1981).

In contrast to the decomposition of acetaldehyde which underwent oxidation to form acetic acid, decomposition of 2-ketones involved C-C bond cleavage to produce alteration products of decreased carbon chain length. Following injection of propene into experiment HMP, the maximum rate of acetic acid production coincided with the maximum in aqueous acetone concentration (Fig. 2c). Subsequent acetone decomposition was accompanied by increases in the concentration of carbon dioxide and acetic acid that were similar in magnitude to the acetone decreases. These trends suggest acetone decomposition occurs via oxidation to produce equal amounts (molal basis) of carbon dioxide and acetic acid. Decomposition of 2-butanone generated after injection of 1-butene into experiment HMP, however, resulted in the production of approximately two moles of acetic acid for each mole of 2-butanone during the period immediately following the maximum in 2-butanone concentration (Fig. 2d). These data suggest that 2-butanone decomposition occurs via cleavage of the interior C-C bond adjacent to the carbonyl group to form two acetic acid molecules. Although similar mass balance is not possible during the PPM experiment due to competing reactions (see below), the production of abundant acetic acid, especially at 350°C, suggests 2-butanone decomposition proceeded through a similar reaction path.

Oxidation of acetic acid produced during oxidative degradation of ethene, propene and 1-butene in the presence of HMP is indicated by the continuous production of CO₂, although decreases in acetic acid concentration were not always apparent due to simultaneous production by oxidation of ketones or acetaldehyde. Complete conversion of acetic acid to carbon dioxide was observed following injection of propene into experiment HMP (HMP-stage 8), which continued for sufficient duration to exhaust the acetic acid source (acetone oxidation).

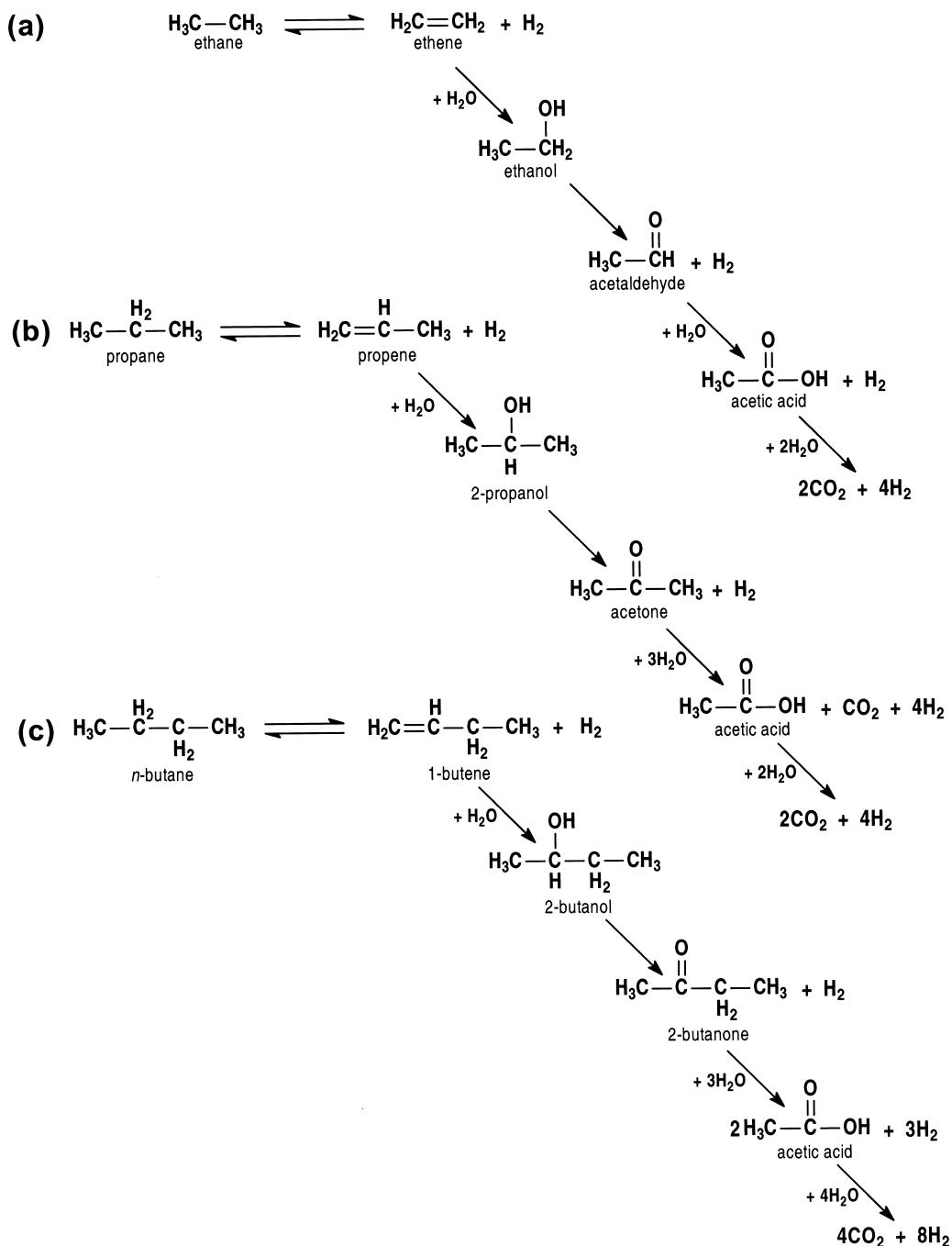


Fig. 8. Schematic representation of reduction, hydration, and oxidation reactions observed during experiments heating (a) aqueous ethane or ethene, (b) aqueous propene, and (c) aqueous 1-butene in the presence of iron-bearing mineral assemblages that buffered redox and the activity of aqueous hydrogen sulfide.

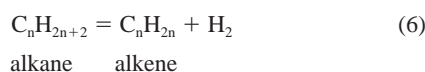
It is generally assumed that decarboxylation to produce equimolar amounts of CH_4 and CO_2 is responsible for acetic acid decomposition under hydrothermal conditions (Carothers and Kharaka, 1978; Kharaka et al., 1983; Palmer and Drummond, 1986; Bell and Palmer, 1994; Bell et al., 1994). Relatively minor amounts of CH_4 production indicates that acetic acid decarboxylation was occurring at a substantially slower rate than oxidation during experiment HMP, resulting in carbon dioxide/methane ratios in excess of 100. This was not the case,

however, during experiment PPM where acetic acid decomposition was accompanied by substantially higher amounts of methane production at all temperatures to produce carbon dioxide/methane ratios of approximately 10. Presently, it is not clear whether differences in the chemical pathways responsible for acetic acid decomposition are due to variations in the redox state of the chemical system or the presence and absence of catalytically active mineral surfaces.

Formation of propionic acid following 1-propene injection

during experiment HMP and, to a greater extent, butyric acid following injection of 1-butene during experiment PPM indicates some oxidation of aqueous *n*-alkenes at the terminal carbon, but at a rate substantially slower than oxidation at the 2 position (Tables 1 and 3). Oxidation of alkenes to their corresponding acids likely involved terminal alcohol and aldehyde intermediaries. The low concentrations of longer chain organic acids notwithstanding, their production demonstrates that reaction paths exist under hydrothermal conditions for the production of C₂₊ organic acids via oxidation of the corresponding *n*-alkane.

Hydration and oxidation reactions that regulate the stability of alkenes will also influence the stability of saturated aqueous hydrocarbons. The generation of ethane, propane, and *n*-butane following injection of the corresponding alkenes during the experiments, as well as the production of ethene following ethane injection, demonstrates that aqueous alkenes and their corresponding aqueous alkanes react reversibly according to the general reaction:



Additional evidence for the reversibility of reaction (6) is provided by decreased ethene concentrations following a reduction in temperature to 300°C during experiment HMP. This decrease is consistent with thermodynamic data for reaction (6) that predict higher ethane/ethene activity ratios for a given H_{2(aq)} activity with decreasing temperature (Johnson et al., 1992). Previous experiments have demonstrated that ethane and ethene may attain a state of reversible redox-dependent thermodynamic equilibrium in the presence of a PPM mineral buffer under hydrothermal conditions (Seewald 1994). Because reaction (6) represents an effective means to generate alkenes from alkanes under hydrothermal conditions, the sequence of reactions responsible for the oxidative decomposition of alkenes may also regulate the abundance of alkanes. Indeed, decreasing propane and *n*-butane concentrations following the initial increases that accompanied injection of propene and 1-butene during experiment HMP at 300°C are consistent with a reversal in the direction of alkane-alkene equilibration via transformations equivalent to reaction (6) as alkene concentrations decreased with time due to oxidative decomposition. Thermal cracking was not responsible for these decreases since such a reaction would produce significant quantities of shorter chain saturated and unsaturated hydrocarbons, which were not observed.

The stepwise oxidation of *n*-alkanes can be represented in general by the sequence of reactions outlined in Figure 9. The formation of terminal alkenes in the first reaction of the sequence is for illustrative purposes only since oxidation of longer chain alkanes may also proceed through the formation of non-terminal alkene intermediaries. The second step involves the specific hydration of the interior carbon associated with the double bond while further oxidation results in the conversion of the hydroxyl functional group to form a ketone. The first three steps of this sequence are analogous to the reaction scheme postulated by Leif and Simoneit (1995) as being responsible for the generation of long chain ketones during hydrous pyrolysis of model compounds and in petroleum and sediment extracts

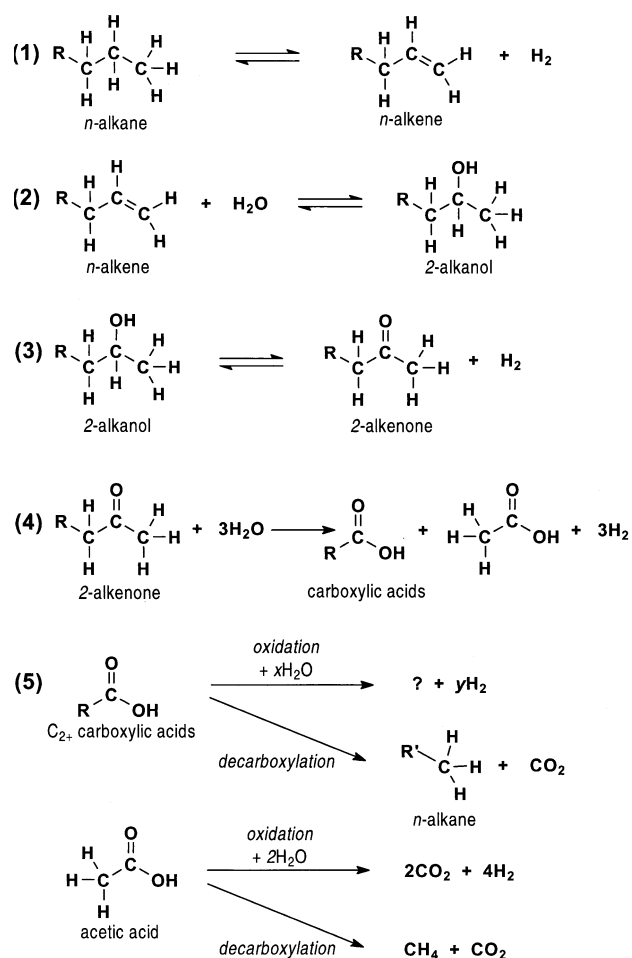


Fig. 9. Generalized reaction scheme for the oxidative decomposition of aqueous *n*-alkanes under hydrothermal conditions.

from the Guaymas Basin hydrothermal system. Additional experimental work demonstrated a key role for long chain alkenes during oxidation and reduction reactions that produce ketones and *n*-alkanes (Leif and Simoneit, 2000). These studies in conjunction with the results presented here demonstrate the general applicability of stepwise oxidation as a mechanism for the decomposition of both long and short-chain hydrocarbons under hydrothermal conditions.

Steps (4) and (5) involve oxidation reactions that produce a decrease in carbon chain length. Oxidation of ketones in the fourth step produces two organic acids and always involves cleavage of the interior C-C bond adjacent to the carbonyl functional group. Two possible reaction paths are indicated in the fifth and final step of the oxidative degradation pathway reflecting variations in the relative rates of acetic acid decarboxylation and oxidation. Experimental results show that both reactions proceed but the relative contribution to acetic acid decomposition varies with redox conditions and/or minerals present. An important feature of the above reaction scheme is that shorter chain *n*-alkanes produced via decarboxylation of C₃₊ organic acids are subject to the same set of stepwise oxidation reactions and will result in the production of additional organic acids. Owing to the specificity of steps (2) and

(4), oxidative decomposition of C₂-C₄ *n*-alkanes can only result in the generation of acetic acid, while C₅₊ *n*-alkanes will produce longer chain acids in addition to acetic acid. Accordingly the occurrence of acetic acid as a major alteration product is an unavoidable consequence of aqueous *n*-alkane oxidation as shorter chain *n*-alkanes accumulate in solution.

Changes in fluid composition during reaction of *n*-heptane with the HMP buffer at 300°C confirm that reactions similar to those responsible for the decomposition of aqueous C₂-C₄ straight chain hydrocarbons influence the stability longer chain compounds. Aqueous *n*-heptane decomposed in the presence of HMP to produce an assemblage of aqueous alteration products dominated by butane, propane, ethane, acetic acid, and carbon dioxide, with conspicuously lower amounts of methane, *n*-pentane and *n*-hexane (Table 2, Fig. 5). This distribution of products can be accounted for by the initial oxidation of *n*-heptane to form *n*-heptenes with the double bond distributed throughout the 1, 2, and 3 positions. Hydration and addition of a carbonyl group to the interior carbon of each double bond followed by oxidative cleavage of the interior C-C bond adjacent to the carbonyl group would produce a series of organic acids with a maximum chain length of five. Indeed, all possible aqueous *n*-heptene and *n*-heptanone isomers and straight chain C₂-C₅ organic acid anions were identified in solution during the HMP experiment. High concentrations of these intermediaries, however, were not realized in solution due to subsequent decomposition reactions and thermodynamic constraints that may limit product/reactant ratios. Decarboxylation of propionic, butyric, and valeric acids during *n*-heptane decomposition is indicated by the generation of a product assemblage containing abundant ethane, propane, *n*-butane and carbon dioxide. Despite considerably higher acetic acid concentrations relative to the other organic acids, the relatively low amounts of methane and abundant carbon dioxide suggests that acetic acid decarboxylation was occurring, but at a substantially slower rate than oxidative decomposition, consistent with the results observed during heating of ethene, propene, and 1-butene in the presence of HMP.

Reaction of *n*-heptane in the presence of the PPM buffer also resulted in greater production of C₁-C₄ *n*-alkanes relative to *n*-pentane and *n*-hexane consistent with decomposition by stepwise oxidation (Fig. 5). In contrast to the HMP experiment, however, considerably less carbon dioxide was generated and methane was the most abundant hydrocarbon. Abundant methane generation indicates an increased rate of acetic acid decarboxylation relative to oxidation in the presence of the PPM buffer.

Formation of saturated hydrocarbons and oxygenated compounds according to the reactions outlined above requires sources of hydrogen and oxygen. Possible sources of hydrogen in the experiments include water and/or the disproportionation of hydrocarbons to form unsaturated products, while sources of oxygen include water and/or magnetite. The production of aqueous hydrogen in response to equilibration of the mineral assemblages with water as well as the absence of large scale formation of unsaturated hydrocarbons suggests that requisite hydrogen for hydrocarbon formation was derived from water during the experiments. Oxygen may also be derived from water during these experiments but cannot be distinguished from magnetite-derived oxygen. This distinction may be of

limited significance, however, since oxygen exchange between magnetite and water readily occurs during equilibration of the fluid with the mineral redox buffer.

The results of these experiments demonstrate that the presence of water and redox sensitive minerals facilitate a variety of reactions that may not be available in dry and/or mineral free environments. Whereas thermal cracking of *n*-alkanes such as *n*-heptane under dry conditions produces a combination of shorter chain saturated hydrocarbons and alkenes (Appleby et al., 1947), aqueous oxidative decomposition produces shorter chain saturated hydrocarbons, carbon dioxide, and abundant acetic acid.

4.2. Thermodynamic Constraints

Although reaction between two chemical species provides direct evidence for a thermodynamic drive and the availability of a suitable reaction mechanism, it is generally not obvious whether a lack of reaction is the result of kinetic barriers or unfavorable thermodynamics. In recent years the enormous growth in the availability of data for the thermodynamic properties of aqueous organic species at elevated temperatures and pressures has provided a framework to address this issue because the energy state of a chemical system can be estimated (Shock and Helgeson, 1990; Helgeson 1992; Shock and Koretsky, 1993; 1995; Schulte and Shock, 1993; Shock 1995; Amend and Helgeson, 1997a,b,c; Helgeson et al., 1998; Richard and Helgeson, 1998; Amend and Helgeson, 2000; Plyasunov and Shock, 2000a; 2000b). The extent to which selected organic reactions may have attained a state of thermodynamic equilibrium was evaluated during the experiments by calculating chemical affinities (*A*) according to the following relationship:

$$A = -RT \ln(Q/K_{eq}) \quad (7)$$

where *R* is the ideal gas constant, *T* is temperature in kelvin, *Q* is the reaction quotient and *K_{eq}* is the equilibrium constant.

Values of *Q* for individual reactions were calculated from measured fluid compositions and the assumption that activity coefficients for all aqueous species are equal to unity. For the purpose of these calculations it was assumed that carbonic and carboxylic acids existed predominantly as fully protonated species. This assumption is only valid at in situ pH values lower than the p*K_a* values of these acids. Although in situ pH cannot be unequivocally determined during these experiments, reaction path modeling using the computer code EQ3/EQ6 (Wolery, 1992; Wolery and Daveler, 1992) predicts that equilibration of deionized water with the HM, HMP and PPM mineral assemblages results in situ pH values of 5.5, 5.0 and 4.9, respectively. Because the p*K_a* values of carbonic and carboxylic acids increase to values > 6 at the temperature and pressure conditions of these experiments, the assumption that organic acid anions exist predominantly as protonated species is appropriate. Values of *K_{eq}* for the reactions considered were calculated from thermodynamic data and equations of state for aqueous organic species, H₂, and H₂O contained in the compilation of Johnson et al. (1992) with additional thermodynamic data from Shock (1995). At thermodynamic equilibrium, *Q* and *K_{eq}* are equal, and expression (7) reduces to zero. Positive affinities indicate that a thermodynamic drive exists for a

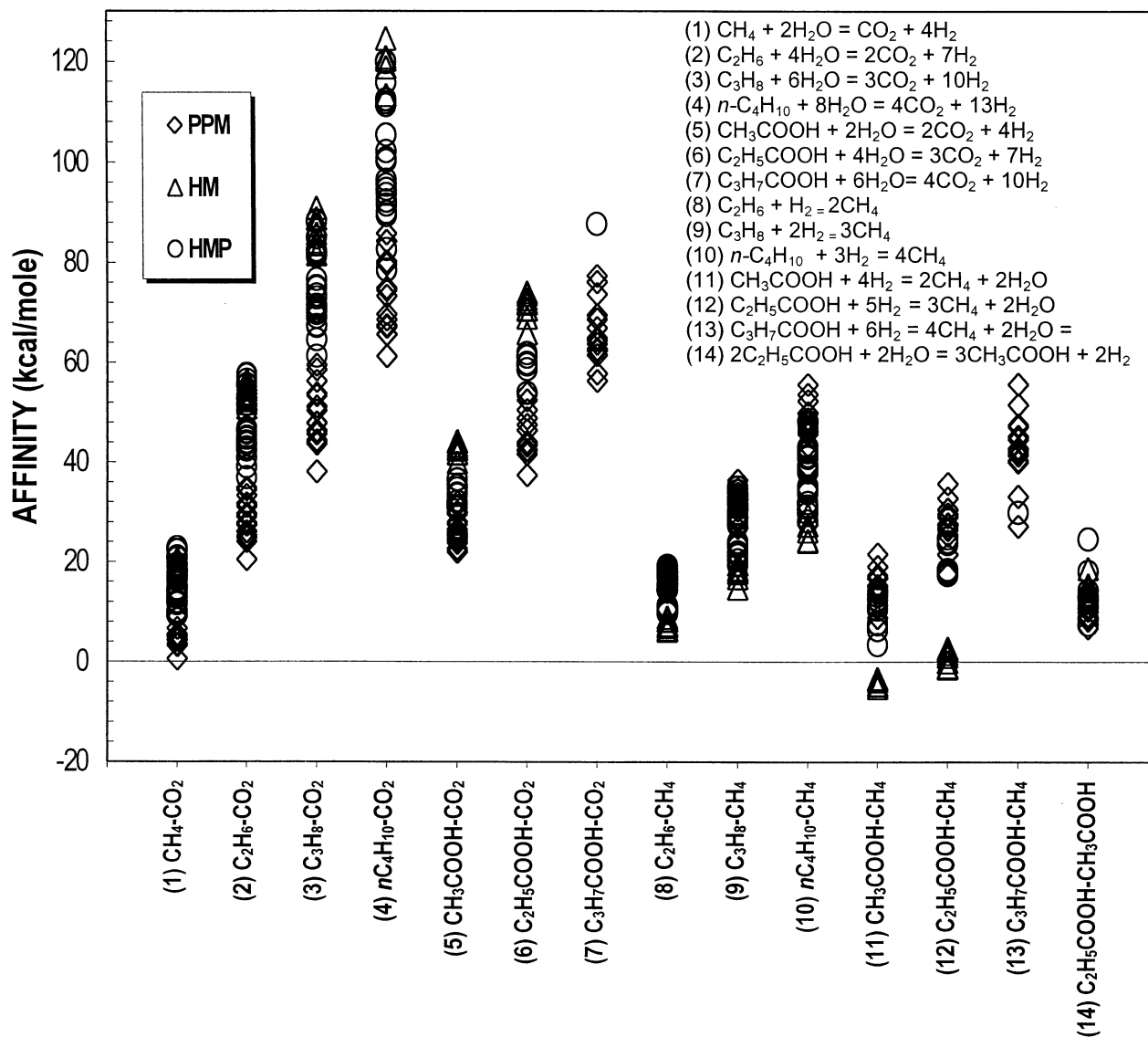


Fig. 10. Calculated chemical affinities for selected redox dependent reactions during experiment PPM (diamonds), HM1 and HM2 (triangles), and HMP (circles). A positive affinity indicates a thermodynamic drive for a reaction to proceed from left to right as written while a negative affinity indicates the opposite.

reaction to proceed from left to right as written while negative affinities indicate the opposite. It is unreasonable to assume that the calculated affinity for a reaction at equilibrium will equal exactly zero due to uncertainties in the thermodynamic and analytical data. Uncertainties in the thermodynamic data used for these calculations are difficult to quantify, but a 1 kcal error in the ΔG_r° for a given reaction is consistent with estimates provided by Shock and Helgeson (1990). In addition, reaction rates become imperceptibly slow as chemical affinities approach zero such that absolute equilibrium may be unattainable on the time scale of these experiments (Aagard and Helgeson, 1982). Accordingly, during this study it has been assumed that calculated affinities of 0 ± 1 kcal are consistent with a state of thermodynamic equilibrium. Other criteria in addition to affinity, however, should be utilized in evaluating the equilibrium state of a chemical system to eliminate the possibility that an

equilibrium fluid composition resulted by chance and was not the result of chemical equilibration. Such criteria include a demonstrated reversibility for a given reaction and a repeated return to an affinity value near zero despite large changes in fluid composition.

Reactions for the production of CO_2 and CH_4 from longer chain hydrocarbons at the redox and temperature conditions of the experiments are characterized by large positive affinities (Fig. 10). Accordingly, the presence of organic compounds at their measured concentrations represents a metastable state created by kinetic barriers that prevent attainment of total thermodynamic equilibrium. Such kinetic barriers, however, do not necessarily preclude individual species from attaining a state of partial metastable equilibrium with other species if a suitable reaction mechanism exists.

The concept of metastable thermodynamic equilibrium has

subsequent temperature increases (Fig. 11a). The calculated affinities reflect a return to constant alkene/ketone molal ratios regulated by the oxidation state of each experiment, despite rapid and large perturbations in the absolute and relative concentrations of each species. In effect, the rate of reaction (9) is sufficiently rapid under the conditions of the PPM and HMP experiments that equilibrium is achieved and maintained in the presence of competing reactions that may produce and/or consume alkenes and ketones. It should be emphasized that equilibration of alkenes and ketones represents a metastable state since thermodynamic data indicate that in the absence of kinetic barriers these species would react to form methane and carbon dioxide (Fig. 10). In addition, because the activity of aqueous hydrogen is buffered by equilibration of the mineral assemblages during these experiments, attainment of redox-dependent metastable thermodynamic equilibrium according to reaction (9) requires that alkenes and ketones are also in a state of metastable equilibrium with respect to water and iron-bearing minerals. These results provide compelling evidence that the role of water and minerals during organic reactions is not limited to catalytic activity, but involves direct participation as reactants in organic transformations.

In addition to alkene-ketone equilibration, alkenes may have approached a state of metastable thermodynamic equilibrium with respect to their corresponding *n*-alkanes according to reaction (6) during some of the experiments. Large negative affinities indicate that reactions involving ethane-ethene, propane-propene, and *n*-butane-1-butene during the 300 and 325°C phases of the PPM experiment continuously approached but did not attain a state of equilibrium (Fig. 12a). It is likely that the slow approach to equilibrium is attributable to the continuous generation of ethene and propene during 1-butene decomposition, and the large amount of reaction required to consume the large reservoir of injected 1-butene. Previous experiments that have demonstrated more rapid ethene-ethane equilibration in the presence of a PPM buffer at 325°C did not include competing reactions that might generate ethene and/or ethane (Seewald, 1994). Increased reaction rates during the 350°C phase of experiment PPM, however, resulted in the rapid exhaustion of ethene, propene, and 1-butene sources. Accordingly, alkene/alkane molal ratios attained or closely approached values consistent with metastable thermodynamic equilibrium in the final sample of this experiment (Fig. 12a).

The above calculations can be used to elucidate reaction pathways involved with 1-butene decomposition during the PPM experiment. Generation of propane, propene, acetone, and propionic acid from 1-butene requires the loss of one carbon unit. The pathway for this process cannot be unequivocally determined from the concentration data alone, but production of substantial carbon dioxide and eventual disappearance of substantial quantities of butyric acid that formed during the early stages of reaction suggests decarboxylation may be responsible. The strong thermodynamic drive to form propane and acetone from propene during this experiment (Figs. 11a and 12a) and the demonstrated availability of suitable reaction mechanisms, suggests that formation of propane and acetone proceeded through reduction and oxidation of a propene intermediary, respectively. Decarboxylation of butyric acid to form propene can be represented by the reaction:

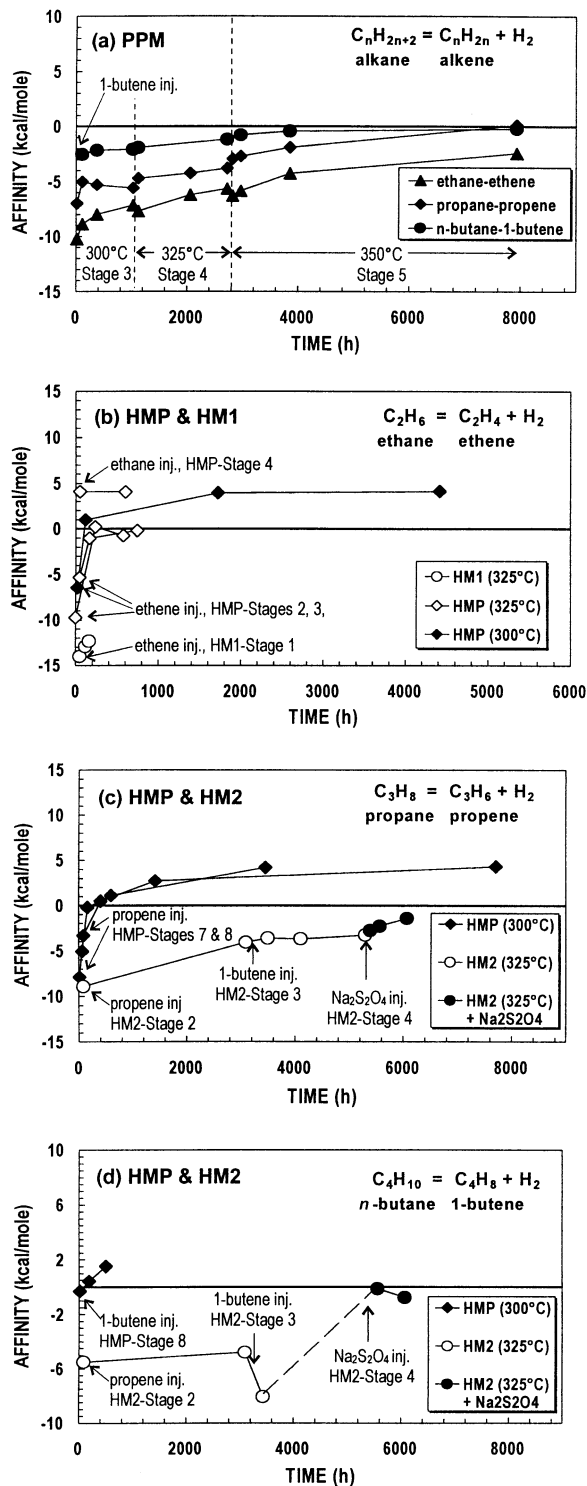
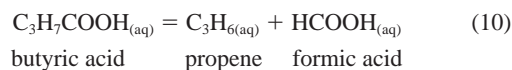


Fig. 12. Calculated chemical affinities for alkane-alkene thermodynamic equilibrium during experiments PPM, HM1, HM2, and HMP. The data are plotted as a function of time elapsed since injection of the indicated species.

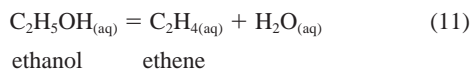


Formic acid generated by this process would rapidly decomposes to CO_2 and H_2 under hydrothermal conditions at the in situ pH of these experiments (McCorm and Seewald, 2001b). Decarboxylation of butyric acid to produce carbon dioxide and propane directly, followed by propane oxidation is not a possible source of propene since there is no thermodynamic drive for reaction (6) to proceed from left to right (Fig. 12a). Similarly, formation of propene from acetone generated by some other process is energetically unfavorable (Fig. 11a).

In general, there was a strong thermodynamic drive for the reaction of alkenes to form alkanes immediately after alkene injection during the HMP experiment (Fig. 12). Rapid consumption of alkenes due to ketone formation (acetaldehyde in the case of ethene), however, resulted in a transition from negative to positive affinities indicating a reversal in the thermodynamically favored direction for reaction (6). Metastable thermodynamic equilibrium (affinity equal to zero) was not attained because the rate of alkene production by alkane oxidation was insufficient to keep pace with alkene consumption due to ketone formation. The transition from negative to positive affinities coincided with a shift from alkane production to alkane consumption. For example, propane concentrations during HMP-stage (8) increased or remained constant in the first three samples analyzed following propene injection before decreasing with continued reaction (Fig. 2c). Calculated affinities for the first three samples were positive while subsequent samples were characterized by negative affinities for reaction (6) (Fig. 12c). The consistency of observed variations in fluid composition with thermodynamic predictions suggests that reaction (6) proceeds readily in both directions facilitating the rapid formation of alkenes from alkanes under hydrothermal conditions.

In contrast to reaction of alkenes at 300°C , reaction of ethene at 325°C did not result in a transition from negative to positive affinities for reaction (6), but instead rapidly approached and maintained a calculated affinity of zero (Fig. 12b). Attainment of ethene-ethane equilibrium at 325°C suggests that the 25°C increase in temperature increased the rate of ethane oxidation to a greater extent than ethene oxidation allowing reaction (6) to maintain equilibrium ethene/ethane ratios despite ethene consumption by acetaldehyde formation. The large positive affinity following ethane injection at 325°C , however, suggests that the shift in relative rates was not sufficient to equilibrate the large reservoir of injected ethane on the time scale of the experiment (Fig. 12b).

Excellent agreement between the predicted equilibrium abundances of ethene and ethanol and observed concentrations during the HM1 experiment at 325°C and HMP experiment at 300°C (Fig. 13) suggests alkene hydration according to the reaction:



is a relatively rapid reaction and may attain a metastable equilibrium state. In contrast to reactions (6) and (9), hydration of alkenes to form alcohols is redox independent. Rapid formation of longer chain 2-alcohols suggests hydration of longer chain alkenes may also attain equilibrium states, although a lack of thermodynamic data for aqueous 2-alcohols at the

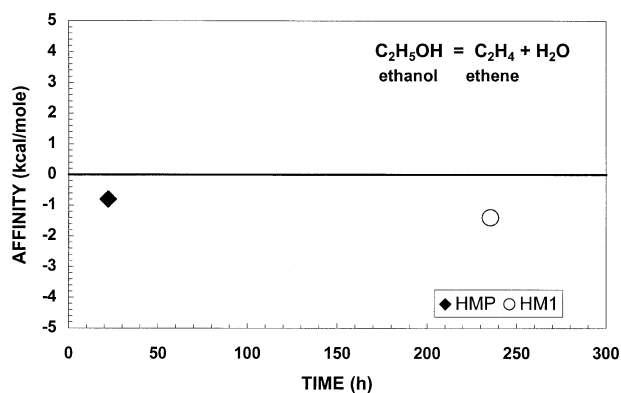


Fig. 13. Calculated chemical affinities for ethene-ethanol thermodynamic equilibrium during experiments HM1 and HMP.

conditions of the experiments precludes a rigorous evaluation of this possibility.

4.3. Role of Sulfur

Although the similarity of aqueous organic compounds produced during the HM, HMP, and PPM experiments indicate similar reaction paths, substantial differences in reaction rates were observed during these experiments. Redox-dependent organic reactions were considerably slower during the sulfur-free stages of the HM experiments relative to HMP experiment, while reaction rates during the PPM experiment were faster than the HM experiments but slower than the HMP experiment. In particular, alkenes injected into experiments HM1 and HM2 persisted at mmolal levels for hundreds of hours in contrast to their relatively rapid disappearance to sub- μmolal abundances during experiments HMP and PPM (Figs. 2, 6 and 7). In addition, decomposition of *n*-alkanes which was observed during experiment HMP at 300°C (Fig. 2) was not observed at 300 or 325°C during experiment PPM or the sulfur-free stages of experiment HM2 and only for *n*-butane during the 350°C stage of experiment PPM (Figs. 6 and 7). Slow reaction rates involving alkenes are also consistent with a lack of alkene-ketone and alkene-alkane equilibration during experiments HM1 and HM2 (Figs. 11 and 12). A rapid increase in the production of alteration products derived from earlier injected propene and 1-butene following injection of sodium thiosulfate into experiment HM2 indicates a substantial increase in the rate of stepwise oxidation (Fig. 7). The differences in reaction rates cannot be attributed to variable thermodynamic drives since the experiments were conducted at identical redox conditions imposed by the presence of hematite and magnetite (Fig. 1). These data point to a strong catalytic role for sulfur species in a broad spectrum of redox dependent reactions involving aqueous organic compounds under hydrothermal conditions. In contrast, rapid thermodynamic equilibration of ethene and ethanol during experiment HM1 suggests that the absence of sulfur may not kinetically inhibit redox independent hydration reactions.

The specific mechanisms and species responsible for the catalytic activity of sulfur are unclear. Measured concentrations of H_2S were below saturation levels for pyrite and pyrrhotite following injection of sodium thiosulfate into experiment HM2

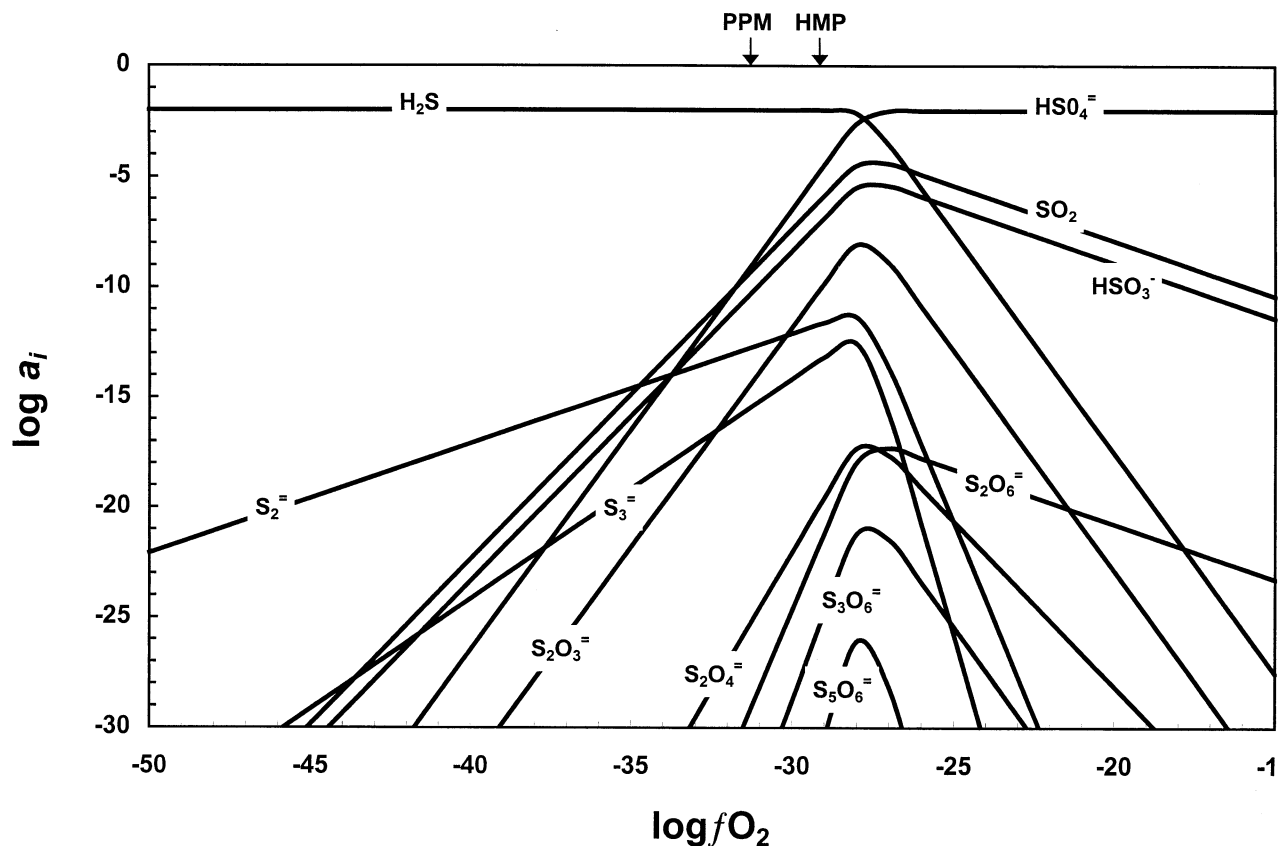


Fig. 14. Calculated activities of selected aqueous sulfur species as a function of redox (fO_2) for a pH 5 fluid containing 10 mmolal total sulfur at 325°C and 350 bars. Requisite thermodynamic data for the construction of this diagram are from the compilation of Johnson et al., (1992). The arrows indicate calculated fO_2 values in equilibrium with a pyrite-pyrrhotite-magnetite (PPM) and a hematite-magnetite-pyrite (HMP) mineral buffer.

(Fig. 1) precludes their presence during this experiment and suggests these minerals are not responsible for catalyzing the observed organic reactions. Magnetite alone does not appear to be catalytically active because it was present in experiments characterized by both rapid and sluggish reaction rates.

The absence of sulfur-bearing minerals in experiments HM2 following sodium thiosulfate addition suggests aqueous sulfur species are responsible for the enhanced reaction rates. The catalytic process may have occurred entirely in solution or as sulfur complexes on the surfaces of minerals. Identifying the specific compounds involved is difficult due to the large number of inorganic and organic sulfur compounds in a variety of oxidation states that may have been present. Because the PPM experiment contained the highest hydrogen sulfide concentrations but was characterized by reaction rates slower than HMP, hydrogen sulfide is not indicated as the catalytically active species. The relative abundance of sulfur species in intermediate oxidation states, however, are strongly dependent on redox (Fig. 14). At fO_2 values of $10^{-29.1}$ and $10^{-31.4}$, consistent with HM and PPM equilibria, respectively, near maximum values in the abundance of sulfur species in intermediate oxidation states are predicted (Fig. 14). Figure 15 shows the activities of aqueous sulfur species during the HMP and PPM experiments at 325°C and 350 bars calculated using measured H_2S abundances and the assumption that in situ pH during both experiments was

5, a value consistent with the results of EQ3/EQ6 reaction path modeling for these systems. Generation of carbon dioxide and organic acids may have influenced pH to some degree during the experiments but this would not have been a large affect

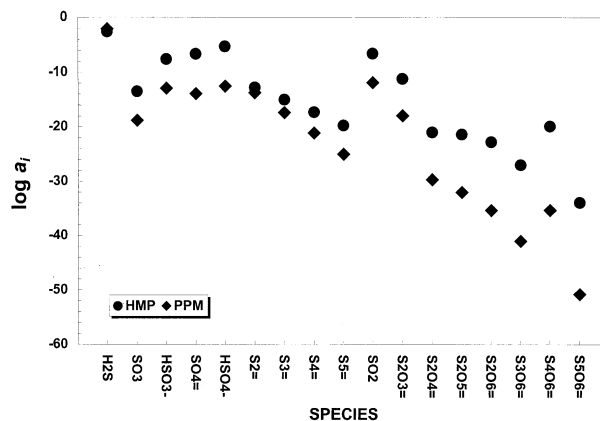


Fig. 15. Calculated activities of selected aqueous sulfur species in equilibrium with a pyrite-pyrrhotite-magnetite (squares) and a hematite-magnetite-pyrite (circles) redox buffer at 325°C, 350 bars, and an in situ pH of 5. Requisite thermodynamic data for the construction of this diagram are from the compilation of Johnson et al., (1992).

since these acids become substantially weaker at temperatures in the vicinity of 325°C. Results of these calculations indicate that despite higher aqueous H₂S concentrations during experiment PPM, the activities of intermediate oxidation state sulfur species are several orders of magnitude lower at equilibrium relative to the HMP experiment. High concentrations of sulfur species in intermediate oxidation states during experiment HMP suggests they may be responsible for enhanced reaction rates relative to the PPM and sulfur-free HM experiments. This result is consistent with other laboratory studies during which sulfur species in intermediate oxidation states were required to facilitate thermochemical sulfate reduction by hydrocarbons (Toland, 1960; Orr, 1982; Goldhaber and Orr, 1995). The possibility also exists that catalytically active aqueous organosulfur compounds may have formed during the experiments but a lack of data for the thermodynamic properties of these species precludes estimation of their stability at the conditions of the experiments.

4.3. Implications for Natural Systems

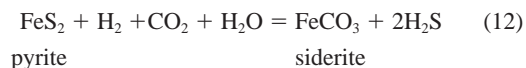
4.3.1. Petroleum stability

Mineral assemblages present in the experiments facilitate the oxidation of hydrocarbons by acting as a sink for generated H₂. Although the redox buffers used are composed of naturally occurring minerals that may be present in sedimentary basins associated with petroleum generation, buffered redox conditions are not a prerequisite for stepwise oxidation. Within the framework of the reaction sequence outlined in Figure 9, a suitable oxidizing agent or a mechanism to remove H₂ is the only requirement. The basic observation that, in general, petroleum reservoirs are spatially separated from source rocks indicates that the generation, expulsion, and migration of hydrocarbons are open-system processes. Thus, there may be ample opportunity for extensive interaction of oil and gas with redox sensitive minerals, despite the absence of these minerals in source and reservoir rocks.

Thermochemical sulfate reduction (TSR) is an example of oxidative oil decomposition that has been well-documented due to the critical role it plays in the formation of sour gas fields and Mississippi Valley-type ore deposits (Krouse et al., 1988; Orr 1974; 1977; Hutcheon et al., 1995; Machel et al., 1995). TSR involves the oxidation of hydrocarbons coupled with the reduction of SO₄²⁻ to H₂S. There is a striking similarity between chemical trends that result from TSR with the results of our experiments in which iron minerals and water represent oxidizing agents. For example, alkanes have been identified as a component of oil that acts as a reducing agent during TSR (Krouse et al., 1988; Hutcheon et al., 1995). In particular, isotopic evidence has been used to demonstrate that TSR results in the oxidation of low molecular weight hydrocarbons such as ethane and propane (Krouse et al., 1988; Hutcheon et al., 1995). Experimental studies have demonstrated that organic acids are initially produced during TSR (Toland et al., 1958) and may subsequently decarboxylate to CO₂ and CH₄ or be oxidized completely to CO₂.

In addition to sulfate in evaporite deposits, there are numerous other oxidizing agents present within sedimentary basins that may react with hydrocarbons. Hematite, magnetite, and

aluminosilicates are all present to varying degrees and contain ferric iron that may be reduced during fluid-rock interaction. Surdam and Crossey (1985) have suggested that ferric iron released during the transformation of smectite to illite may oxidize organic matter to produce organic acids. In a separate study, Surdam et al. (1993) suggest that reduction of hematite in red sandstone petroleum reservoirs may also generate significant amounts of organic acids. Moreover, pyrite which is abundant in reducing organic-rich sediments represents an effective oxidizing agent as sulfur is present in the -I oxidation state and can be further reduced. Thus, pyrite alteration to form minerals such as siderite according to the reaction:



represents an effective means to consume H₂ generated by *n*-alkane oxidation. Extensive alteration of inorganic sediment components and formation of ferrous iron phases such as chlorite and siderite at temperatures associated with the generation of oil and natural gas indicates that ferric iron and pyrite sulfur in sediments are reactive oxidizing agents available for the oxidative decomposition of hydrocarbons in subsurface environments. In addition, water is not just a solvent in the reactions described above but also represents an oxidizing agent. In the absence of a mechanism to remove H₂, reducing conditions would quickly develop as H₂ accumulates in solution, creating a decreased thermodynamic drive for oxidative decomposition. Relatively rapid diffusion rates for H₂, however, may allow it to preferentially diffuse out of petroleum reservoirs thereby maintaining a thermodynamic drive for the oxidation of hydrocarbons by an essentially inexhaustible supply of water. Thus, although TSR is the most obvious and well-studied case of oxidative hydrocarbon decomposition in sedimentary basins, it represents only one example of the numerous redox dependent processes involving inorganic sedimentary components, all of which may influence the stability of oil and the generation of oxygenated alteration products and natural gas.

The redox dependence of hydrocarbon stability in aqueous environments indicates that the stability of oil is not simply a function of time and temperature alone. Oxidative hydrocarbon decomposition requires the availability of suitable oxidizing agents and water and is catalyzed by sulfur species. One can easily envision a scenario where the presence of water and ferric and/or oxidized sulfur-bearing minerals provides a reaction path for rapid oil decomposition while the same oil in the absence of sulfur catalysts, oxidizing agents and/or water could persist for considerably longer periods of time at higher temperatures. Such a model may account for the presence of oil in a variety of environments at temperatures higher than conventional models would predict (Price, 1993).

4.3.2. Natural gas composition

Despite the production of enormous quantities of natural gas throughout the world and its economic and environmental significance, factors that control the generation of natural gas remain poorly understood. Until recently, conventional wisdom has advocated that thermal cracking of kerogen and/or oil

results in the production of thermogenic natural gas (Tissot and Welte, 1984; Barker, 1990; Ungerer, 1990; Hunt, 1996). In this model, a mixture of oil and gas is generated at low thermal stress, followed by thermal decomposition of generated oil as time and temperature increase with progressive burial. In the endmember case at high thermal stress, these processes are believed to result in the formation of dry gas (gas in which the hydrocarbon fraction is composed almost entirely of CH_4) due to the complete thermal destruction of C_{2+} hydrocarbons. Convincing arguments have been made, however, to suggest that a purely thermal model cannot account for the absence of C_{2+} hydrocarbons in dry gas (Mango et al., 1994; Mango 1997). Specifically, thermal cracking of kerogen and individual long-chain hydrocarbons produces a gas that is relatively enriched in $\text{C}_2\text{-C}_4$ hydrocarbons (i.e., a wet gas). Exceedingly sluggish reaction rates for the thermal cracking of low molecular weight hydrocarbons at temperatures typically associated with the generation of natural gas suggests that dry gas does not form by the thermal decomposition of C_{2+} hydrocarbons in wet gas (see Mango, 1997, for a thorough review).

The inability of a purely thermal model to account for the composition of dry gas has prompted researchers to propose a variety of new models for its origin. On the basis of laboratory experiments, Mango et al. (1994) have suggested that transition metal catalysis during the decomposition of long-chain hydrocarbons is essential for the production of dry gas. In contrast, Price and Schoell (1995) have suggested that natural gas initially contains a significant fraction of C_{2+} hydrocarbons at the site of generation but becomes enriched in CH_4 in response to fractionation processes during expulsion and migration. Other researchers have hypothesized that an almost pure CH_4 gas is generated from residual kerogen due to demethylation of aromatic moieties after the majority of oil has been generated and expelled (McNeil and BeMent, 1996). Although these models cover a wide range of possible mechanisms, they are limited by consideration of reactions involving only organic species as chemical reactants.

The experiments presented here demonstrate that water and iron-bearing minerals participate in chemical reactions responsible for the decomposition of C_{2+} hydrocarbons at elevated temperatures and pressures. Such reactions may be responsible for the production of dry natural gas in sedimentary basin since kinetic barriers to the oxidation of short chain n -alkanes are sufficiently low that oxidative decomposition at 300°C can be observed within a laboratory time scale of hundreds to thousands of hours. This result indicates that oxidative degradation is substantially faster than thermal cracking. For example, at 300°C the calculated half life of propane decomposition by thermal cracking is 3300 y (Laidler et al., 1962), considerably longer than propane decomposition in the presence of a hematite-magnetite-pyrite mineral assemblage that is characterized by a half life of approximately two years (Fig. 2c). Similar rates of reaction were observed for the decomposition of ethane and n -butane (Figs. 2b,d). Thus stepwise oxidation may play a critical role during the conversion of wet gas to dry gas by selectively degrading C_{2+} n -alkanes. The rate of this process is strongly dependent on the geochemical environment in addition to time and temperature since the abundances of reaction intermediaries are strongly redox dependent (Fig. 9). In particular, alkene formation may represent the rate limiting step during

n -alkane oxidation due to thermodynamic constraints that limit alkane/alkene ratios to very large values under reducing redox conditions likely to exist in sedimentary basins associated with oil and natural gas generation (Shock and Helgeson, 1990).

A key factor influencing the amounts and composition of a CH_4 -rich natural gas are the reactions responsible for the decomposition of acetic acid. Complete oxidation results in the production of two moles of CO_2 for each mole of acetic acid while decarboxylation produces equal amounts of CH_4 and CO_2 . Accordingly, decarboxylation as the final step during the oxidative decomposition of n -alkanes would produce CH_4 during the evolution of "wet" gas to "dry" gas in contrast to oxidation which would simply remove C_{2+} hydrocarbons leaving residual CH_4 .

4.3.3. Mass balance constraints on the generation of hydrocarbons and oxygenated alteration products

It has long been assumed that hydrogen and oxygen in oil and natural gas are derived solely from kerogen. This assumption, along with information on the variations in the elemental composition of kerogen with increasing thermal maturity, has been used to predict the composition, amounts, and timing of organic alteration products generated in sedimentary basins (Tissot and Welte, 1984; Cooles et al., 1986; Barker 1990; Ungerer, 1990). The participation of water and minerals in organic reactions, however, indicates that hydrogen and oxygen are available from inorganic sources, so that constraints placed on the amounts and relative timing of oil, natural gas, and organic acids that are based on the compositional evolution of kerogen may not be appropriate.

Derivation of oxygen from water has profound implications for the generation of organic acids and carbon dioxide in petroleum producing basins. These species have been the focus of extensive research because they are weak acids and may be responsible for enhancing porosity in petroleum migration conduits and reservoirs. In addition, carbon dioxide represents an essential ingredient for the formation of carbonate cements that may destroy porosity. The observation that large decreases in kerogen oxygen content are not accompanied by hydrogen decreases during early-stage maturation has been routinely used as evidence to suggest that organic acids and carbon dioxide formation precede the onset of oil generation. Generation of carbon dioxide and carboxylic acids containing water-derived oxygen during n -alkane oxidation suggests that oxygenated alteration products may be generated before, during, and after peak oil generation in quantities substantially greater than models limited by kerogen oxygen content would predict. Consistent with this suggestion are the results of Monterey Shale hydrous pyrolysis experiments that have demonstrated extensive conversion of organic carbon to carbon dioxide following peak oil generation (Seewald et al., 1998).

It has been argued that organic acids will have a minimal effect on reservoir porosity because alteration minerals present in source rocks and along migration pathways will consume acidity created by organic acids before reaching the reservoir (Giles et al., 1994). This argument assumes that all organic acids are generated directly from kerogen located in source rocks. The generation of organic acids from aqueous n -alkanes indicates organic acids can be generated subsequent to oil

expulsion and may even occur in petroleum reservoirs provided a suitable oxidizing agent is present. Accordingly, although titration of organic acids in source rocks and migration conduits is likely, it may not limit the potential role organic acids may play in developing reservoir porosity.

As is the case for the formation of oxygenated organic alteration products, derivation of requisite hydrogen from water during the formation of saturated hydrocarbons suggests kerogen hydrogen content places few constraints on the hydrocarbon generation potential of a sedimentary basin. Because petroleum generation occurs via the cleavage of intact kerogen fragments to form high molecular weight saturated alteration products, the hydrogen demand is relatively minor and does not represent a limiting factor in the amount of oil generated. With increasing maturation, however, the average chain length decreases and the H/C molal ratio decreases from a value of two in a hypothetical saturated hydrocarbon of infinite chain length to four in methane. This process requires a substantial addition of hydrogen and the almost infinite supply of water-derived hydrogen in sedimentary basins suggests hydrogen availability may not be a limiting factor.

5. SUMMARY

Results of mineral buffered laboratory experiments indicate that aqueous reactions involving straight chain hydrocarbons and their alteration products respond systematically, and in some cases reversibly, to variations in the redox state of the chemical system. Under redox buffered conditions, decomposition of aqueous *n*-alkanes proceeds through a sequence of oxidation, hydration, and decarboxylation reactions. Reaction intermediaries in order of formation include alkenes, alcohols, ketones, and organic acids, that ultimately react to form carbon dioxide and shorter chain saturated hydrocarbons. This alteration assemblage is compositionally distinct from that produced by purely thermal processes under anhydrous conditions, indicating that the presence of water and minerals provide alternative reaction pathways for the decomposition of hydrocarbons.

The rate of hydrocarbon oxidation decreases substantially under reducing redox conditions and in the absence of catalytically active aqueous sulfur. These results represent compelling evidence that the stability of organic species at elevated temperatures is not simply a function of time and temperature alone. In sedimentary basins, the absence or presence of suitable oxidizing agents such as water and catalytically active sulfur species will influence the stability of petroleum at elevated temperatures and pressures, and may account for the persistence of oil at temperatures higher than conventional models predict. Oxidative decomposition has profound implications for the composition of natural gas since oxidation of low molecular weight (C₂-C₄) saturated hydrocarbons may occur faster than thermal cracking under the appropriate conditions, providing a mechanism for the formation of methane-rich natural gas.

Thermodynamic evaluation of alteration products during the experiments indicates that metastable alkane-alkene, alkene-ketone, and alkene-alcohol thermodynamic equilibrium may be attained under hydrothermal conditions. This equilibrium includes water and iron-bearing minerals, demonstrating the di-

rect involvement of inorganic species as reactants during organic transformations. The high reactivity of water and iron-bearing minerals suggests that they represent abundant sources of hydrogen and oxygen available for the formation of hydrocarbons and oxygenated alteration products. Thus, variations in elemental kerogen composition may not accurately reflect the timing and extent of hydrocarbon, carbon dioxide, and organic acid generation in sedimentary basins.

Due to the close association of water, minerals, and organic matter in sedimentary basins, organic-inorganic interactions are an unavoidable consequence during sediment alteration. Accordingly, models that do not integrate both organic and inorganic geochemical processes may not accurately predict the stability and compositional evolution of organic species in subsurface environments.

Acknowledgments—Funds to support this research were provided by the National Science Foundation (Grant OCE-9618179). Numerous discussions with Anna Cruse, Tom McCollom, and Peter Saccocia were invaluable during the preparation of this manuscript. Insightful and helpful reviews by Hal Helgeson, Roald Leif, and Laura Crossey are appreciated. WHOI contribution no. 10378.

Associate editor: J. B. Fein

REFERENCES

- Aagard P. and Helgeson H. C. (1982) Thermodynamic and kinetic constraints on reaction rates among minerals and aqueous solutions. I. theoretical considerations. *Am. J. Sci.* **282**, 237–285.
- Amend J. P. and Helgeson H. C. (1997a) Calculation of the standard molal thermodynamic properties of aqueous biomolecules at elevated temperatures and pressures. 1. L- α -amino acids. *J. Chem. Soc., Far. Trans.* **93**, 1927–1941.
- Amend J. P. and Helgeson H. C. (1997b) Group additivity equations of state for calculating the standard molal thermodynamic properties of aqueous organic molecules at elevated temperatures and pressures. *Geochim. Cosmochim. Acta* **61**, 11–46.
- Amend J. P. and Helgeson H. C. (1997c) Solubilities of the common L- α -amino acids as a function of temperature and solution pH. *Pure Appl. Chem.* **69**, 935–942.
- Amend J. P. and Helgeson H. C. (2000) Calculation of the standard molal thermodynamic properties of aqueous biomolecules at elevated temperatures and pressures. II. Unfolded proteins. *Biophys. Chem.* **84**, 105–136.
- Appleby W. G., Avery W. H., and Meerbott W. K. (1947) Kinetics and mechanism of the thermal decomposition of *n*-heptane. *J. Am. Chem. Soc.* **69**, 2279–2285.
- Barker C. (1990) Calculated volume and pressure changes during the thermal cracking of oil to gas in reservoirs. *Am. Assoc. Petrol. Geol. Bull.* **74**, 1254–1261.
- Bell J. L. S. and Palmer D. A. (1994) Experimental studies of organic acid decomposition. In *Organic Acids in Geological Processes* (eds. E. D. Pittman and M. D. Lewan). Springer-Verlag, New York. pp. 226–269.
- Bell J. L. S., Palmer D. A., Barnes H. L., and Drummond S. E. (1994) Thermal-decomposition of Acetate. 3. Catalysis by mineral surfaces. *Geochim. Cosmochim. Acta* **58**, 4155–4177.
- Carothers W. W. and Kharaka Y. K. (1978) Aliphatic acid anions in oil-field waters—implications for origin of natural gas. *Am. Assoc. Pet. Geol. Bull.* **62**, 2441–2453.
- Cooles G. P., Mackenzie A. S., and Quigley T. M. (1986) Calculation of petroleum masses generated and expelled from source rocks. *Org. Geochem.* **10**, 235–245.
- Douglas A. G. and Mair B. J. (1965) Sulfur: Role in genesis of petroleum. *Science* **147**, 499–501.
- Eglinton T. I., Curtis C. D., and Rowland S. J. (1987) Generation of water-soluble organic acids from kerogen during hydrous pyrolysis: Implications for porosity development. *Min. Mag.* **51**, 495–503.

- Giles M. R., de Boer R. B., and Marshall J. D. (1994) How important are organic acids in generating secondary porosity in the subsurface? In *Organic Acids in Geological Processes* (eds. E. D. Pittman and M. D. Lewan). Springer-Verlag, New York. pp. 449–470.
- Goldhaber M. B. and Orr W. L. (1995) Kinetic controls on thermochemical sulfate reduction as a source of sedimentary H₂S. In *Geochemical Transformations of Sedimentary Sulfur* (eds. M. A. Vairavamurthy and M. A. A. Schoonen). Am. Chem. Soc., Wash. D.C., pp. 412–425.
- Helgeson H. C. (1991) Organic/inorganic reactions in metamorphic processes. *Can. Min.* **29**, 707–739.
- Helgeson H. C. (1992) Calculation of the thermodynamic properties and relative stabilities of aqueous acetic and chloroacetic acids, acetate and chloroacetates, and acetyl and chloroacetyl chlorides at high and low temperatures and pressures. *Appl. Geochim.* **7**, 1089–1198.
- Helgeson H. C. (1999) Thermodynamic prediction of the relative stabilities of hyperthermophilic enzymes. In *Chem. Thermodyn.* (ed. T. M. Letcher), Blackwell Science Ltd., Oxford, pp. 301–312.
- Helgeson H. C., Knox A. M., Owens C. E., and Shock E. L. (1993) Petroleum, oil field waters, and authigenic mineral assemblages: Are they in metastable equilibrium in hydrocarbon reservoirs? *Geochim. Cosmochim. Acta* **57**, 3295–3339.
- Helgeson H. C., Owens C. E., Knox A. M., and Richard L. (1998) Calculation of the standard molal thermodynamic properties of crystalline, liquid, and gas organic molecules at high temperatures and pressures. *Geochim. Cosmochim. Acta* **62**, 985–1081.
- Hoering T. C. (1984) Thermal reaction of kerogen with added water, heavy water, and pure organic substances. *Org. Geochem.* **5**, 267–278.
- Hunt J. M. (1996) *Petroleum Geochemistry and Geology*. W. H. Freeman and Co., New York.
- Hutcheon I., Krouse H. R., and Abercrombie H. J. (1995) Controls on the origin and distribution of elemental sulfur, H₂S, and CO₂ in Paleozoic hydrocarbon reservoirs in Western Canada. In *Geochemical Transformations of Sedimentary Sulfur* (eds. M. A. Vairavamurthy and M. A. A. Schoonen). Am. Chem. Soc., Wash. D. C., pp. 426–438.
- Johnson J. W., Oelkers E. H., and Helgeson H. C. (1992) SUPCRT92: Software package for calculating the standard molal thermodynamic properties of minerals, gases, aqueous species, and reactions among them as functions of temperature and pressure. *Comp. Geo.* **18**, 899–947.
- Kharaka Y. K., Carothers W. W., and Rosenbauer R. J. (1983) Thermal decarboxylation of acetic acid: Implications for origin of natural gas. *Geochim. Cosmochim. Acta* **47**, 397–402.
- Krouse H. R., Viau C. A., Eliuk L. S., Ueda A., and Halas S. (1988) Chemical and isotopic evidence of thermochemical sulphate reduction by light hydrocarbon gases in deep carbonate reservoirs. *Nature* **333**, 415–419.
- Laidler K. J., Sagert N. H., and Wojciechowski B. W. (1962) Kinetics and mechanisms of the thermal decomposition of propane. *Proc. Royal Soc. London* **A270**, 242–253.
- Leif R. N. and Simoneit B. R. T. (1995) Ketones in hydrothermal petroleum and sediment extracts from Guaymas Basin, Gulf of California. *Org. Geochem.* **23**, 889–904.
- Leif R. N. and Simoneit B. R. T. (2000) The role of alkenes produced during hydrous pyrolysis of a shale. *Org. Geochem.* **31**, 1189–1208.
- Lewan M. D. (1997) Experiments on the role of water in petroleum formation. *Geochim. Cosmochim. Acta* **61**, 3691–3723.
- Lewan M. D. (1998) Sulfur-radical control on rates of natural petroleum formation. *Nature* **391**, 164–166.
- Machel H. G., Krouse H. R., Riciputi L. R., and Cole D. R. (1995) Devonian nisku sour gas play, Canada: a unique natural laboratory for study of thermochemical sulfate reduction. In *Geochemical Transformations of Sedimentary Sulfur* (eds. M. A. Vairavamurthy and M. A. A. Schoonen). Am. Chem. Soc., Wash. D. C., pp. 439–454.
- Mango F. D. (1997) The light hydrocarbons in petroleum: A critical review. *Org. Geochem.* **26**, 417–440.
- Mango F. D., Hightower J. W., and James A. T. (1994) Catalysis in the origin of natural gas. *Nature* **368**, 536–538.
- McCullom T. M., Ritter G., and Simoneit B. R. T. (1999a) Lipid synthesis under hydrothermal conditions by Fischer-Tropsch-type reactions. *Orig. Life Evol. Bios.* **29**, 153–166.
- McCullom T. M. and Seewald J. S. (2001a) Reactivity of monocyclic aromatic compounds under hydrothermal conditions. *Geochim. Cosmochim. Acta* **65**, 455–468.
- McCullom T. M. and Seewald J. S. (2001b) A reassessment of the potential for reduction of dissolved CO₂ during serpentinization of olivine. *Geochim. Cosmochim. Acta* (in press).
- McCullom T. M., Simoneit B. R. T., and Shock E. L. (1999b) Hydrous pyrolysis of polycyclic aromatic hydrocarbons and implications for the origin of PAH in hydrothermal petroleum. *Energy & Fuels* **13**, 401–410.
- McNeil R. I. and BeMent W. O. (1996) Thermal stability of hydrocarbons: Laboratory criteria and field examples. *Energy & Fuels* **10**, 60–67.
- Orr, W. L. (1974) Changes in sulfur content and isotopic ratios of sulfur during petroleum maturation; study of Big Horn Basin Paleozoic oils, advances in petroleum geochemistry. *Am. Ass. Petrol. Geol. Bull.* **58**, 2295–2318.
- Orr W. L. (1977) Geologic and geochemical controls on the distribution of hydrogen sulfide in natural gas. In *Adv. Org. Geochem. 1975* (eds. R. Campo and J. Goni). Enadimsa, Madrid. pp. 572–597.
- Orr W. L. (1982) Rate and mechanism of non-microbial sulfate reduction. *Geol. Soc. Am. Abs. Prog.* **14**, 580.
- Palmer D. A. and Drummond S. E. (1986) Thermal decarboxylation of acetate. Part I. The kinetics and mechanism of reaction in aqueous solution. *Geochim. Cosmochim. Acta* **50**, 813–823.
- Plyasunov A. V. and Shock E. L. (2000a) Thermodynamic functions of hydration of hydrocarbons at 298.15 K and 0.1 MPa. *Geochim. Cosmochim. Acta* **63**, 439–468.
- Plyasunov A. V. and Shock E. L. (2000b) Standard state Gibbs energies of hydration of hydrocarbons at elevated temperatures as evaluated from experimental phase equilibria studies. *Geochim. Cosmochim. Acta* **64**, 2811–2833.
- Pokrovski V. A. and Helgeson H. C. (1994) Solubility of petroleum in oil-field waters as a function of the oxidation state of the system. *Geology* **22**, 851–854.
- Price L. C. (1981) Aqueous solubility of crude oil to 400°C and 2,000 bars pressure in the presence of gas. *J. Pet. Geol.* **4**(2), 195–223.
- Price L. C. (1993) Thermal stability of hydrocarbons in nature: Limits, evidence, characteristics, and possible controls. *Geochim. Cosmochim. Acta* **57**, 3261–3280.
- Price L. C. and Schoell M. (1995) Constraints on the origins of hydrocarbon gas from compositions of gases at their site of origin. *Nature* **378**, 368–371.
- Price L. C. and Wenger L. M. (1992) The influence of pressure on petroleum generation and maturation as suggested by aqueous pyrolysis. *Org. Geochem.* **19**, 141–159.
- Richard L. and Helgeson H. C. (1998) Calculation of the thermodynamic properties at elevated temperatures and pressures of saturated and aromatic high molecular weight solid and liquid hydrocarbons in kerogen, bitumen, petroleum, and other organic matter of biogeochemical interest. *Geochim. Cosmochim. Acta* **62**, 3591–3636.
- Schulte M. D. and Shock E. L. (1993) Aldehydes in hydrothermal solution: Standard partial molal thermodynamic properties and relative stabilities at high temperatures and pressures. *Geochim. Cosmochim. Acta* **57**, 3835–3846.
- Seewald J. S. (1994) Evidence for metastable equilibrium between hydrocarbons under hydrothermal conditions. *Nature* **370**, 285–287.
- Seewald J. S. (1997) Mineral redox buffers and the stability of organic compounds under hydrothermal conditions. *Mat. Res. Soc. Symp. Proc.* **432**, 317–331.
- Seewald J. S., Benitez-Nelson B. C., and Whelan J. K. (1998) Laboratory and theoretical constraints on the generation and composition of natural gas. *Geochim. Cosmochim. Acta* **62**, 1599–1617.
- Seyfried W. E. Jr., Janecky D. R. and Berndt M. E. (1987) Rocking autoclaves for hydrothermal experiments. II. The flexible reaction-cell system. In *Hydrothermal Experimental Techniques* (eds. G. C. Ulmer and H. L. Barnes). John Wiley and Sons, New York. pp. 216–240.
- Shock E. L. (1988) Organic acid metastability in sedimentary basins. *Geol.* **16**, 886–890.

- Shock, E. L. (1989) Corrections to "Organic acid metastability in sedimentary basins." *Geol.* **17**, 572–573.
- Shock, E. L. (1994) Application of thermodynamic calculations to geochemical processes involving organic acids. In *Organic Acids in Geological Processes* (eds. E. D. Pittman and M. D. Lewan). Springer-Verlag, New York. pp. 270–318.
- Shock, E. L. (1995) Organic acids in hydrothermal solutions: Standard molal thermodynamic properties of carboxylic acids, and estimates of dissociation constants at high temperatures and pressures. *Am. J. Sci.* **295**, 496–580.
- Shock E. L. and Helgeson H. C. (1990) Calculation of the thermodynamic and transport properties of aqueous species at high pressures and temperatures: Standard partial molal properties of organic species. *Geochim. Cosmochim. Acta* **54**, 915–945.
- Shock E. L. and Koretsky C. M. (1993) Metal-organic complexes in geochemical processes: Calculation of standard partial molal thermodynamic properties of aqueous acetate complexes at high pressures and temperatures. *Geochim. Cosmochim. Acta* **57**, 4899–4922.
- Shock, E. L. and Koretsky, C. M. (1995) Metal-organic complexes in geochemical processes: Estimation of standard partial molal thermodynamic properties of aqueous complexes between metal cations and monovalent organic acid ligands at high pressures and temperatures. *Geochim. Cosmochim. Acta* **59**, 1497–1532.
- Siskin M. and Katritzky A. R. (1991) Reactivity of organic compounds in hot water: Geochemical and technological implications. *Science* **254**, 231–237.
- Stalker L., Farrimond P., and Larter S. R. (1994) Water as an oxygen source for the production of oxygenated compounds (including CO₂ precursors) during kerogen maturation. *Adv. Org. Geochem. 1993*, *Org. Geochem.* **22**, 477–486.
- Streitwieser, Jr., A. and Heathcock C. H. (1981) Introduction to Organic Chemistry. Macmillan Publishing Co., Inc., New York.
- Surdam, R. C. and Crossey, L. J. (1985) Organic-inorganic reactions during progressive burial: Key to porosity and permeability enhancement and preservation. *Phil. Trans. Roy. Soc. London* **A315**, 135–156.
- Surdam R. C., Jiao Z. S., and MacGowan D. B. (1993) Redox reactions involving hydrocarbons and mineral oxidants: A mechanism for significant porosity enhancement in sandstones. *Am. Assoc. Petrol. Geol. Bull.* **77**, 1509–1518.
- Tannenbaum E., Huizinga, R. J. and Kaplan, I. R. (1986) Role of minerals in thermal alteration of organic matter-II: A material balance. *Am. Assoc. Petrol. Geol. Bull.* **70**, 1156–1165.
- Tissot B. P. and Welte D. H. (1984) Petroleum Formation and Occurrence. Springer-Verlag, New York.
- Toland W. G. (1960) Oxidation of organic compounds with aqueous sulfate. *J. Am. Chem. Soc.* **82**, 1911–1916.
- Toland W. G., Hagman D. L., Wilkes J. B., and Brutschy F. J. (1958) Oxidation of organic compounds with aqueous base and sulfur. *J. Am. Chem. Soc.* **80**, 5423–5427.
- Toulmin P. III. and Barton P. B. (1964) A thermodynamic study of pyrite and pyrrhotite. *Geochim. Cosmochim. Acta* **28**, 641–671.
- Ungerer P. (1990) State of the art research in kinetic modeling of oil formation and expulsion. *Org. Geochem.* **16**, 1–25.
- Wolery T. J. (1992) EQ3NR, A computer Program for Aqueous Speciation-Solubility Calculations: Theoretical Manual, User's Guide, and Related Documentation. Lawrence Livermore National Lab.
- Wolery T. J. and Daveler S. A. (1992) EQ6, A Computer Program for Reaction Path Modeling of Aqueous Geochemical Systems: Theoretical Manual, User's Guide, and Related Documents. Lawrence Livermore National Lab.